Brain, Behavior, and Immunity 127 (2025) 287–302

Contents lists available at ScienceDirect

Brain Behavior and Immunity

journal homepage: www.elsevier.com/locate/ybrbi

Full-length Article

The schizophrenia-associated gene *CSMD1* encodes a complement classical pathway inhibitor predominantly expressed by astrocytes and at synapses in mice and humans

Robert A.J. Byrne [a,b,c,*], Jacqui Nimmo [b,c], Megan Torvell [b,c], Sarah M. Carpanini [b,c], Nikoleta Daskoulidou [b,c], Timothy R. Hughes [c], Lucy V. Noble [b,c], Aurora Veteleanu [b,c], Lewis M. Watkins [b,c], Wioleta M. Zelek [b,c], Michael C. O'Donovan [a,d], Bryan Paul Morgan [a,b,c,**]

[a] Hodge Centre for Neuropsychiatric Immunology, School of Medicine, Cardiff University, Hadyn Ellis Building, Maindy Road, Cardiff, Wales CF24 4HQ, UK
[b] UK Dementia Research Institute, School of Medicine, Cardiff University, Hadyn Ellis Building, Maindy Road, Cardiff, Wales CF24 4HQ, UK
[c] Division of Infection and Immunity, School of Medicine, Cardiff University, Henry Wellcome Building, Heath Park, Cardiff, Wales CF14 4XN, UK
[d] Centre for Neuropsychiatric Genetics and Genomics, School of Medicine, Cardiff University, Hadyn Ellis Building, Maindy Road, Cardiff, Wales CF24 4HQ, UK

ARTICLE INFO

Keywords:
CSMD1
Complement
Schizophrenia
Monoclonal Antibody

ABSTRACT

CUB and sushi multiple domains 1 (*CSMD1*) is predominantly expressed in brain and robustly associated with schizophrenia risk; however, understanding of which cells express CSMD1 in brain and how it impacts risk is lacking. *CSMD1* encodes a large transmembrane protein including fifteen tandem short consensus repeats (SCRs), resembling complement C3 convertase regulators. CSMD1 complement regulatory activity has been reported and mapped to SCR17-21. We expressed two SCR domains of CSMD1, SCR17-21 and SCR23-26, and characterised their complement regulatory activity using a panel of functional assays testing convertase and terminal pathway inhibition. Both domains inhibited the classical pathway C3 convertase by acting as factor I cofactors; neither domain caused any inhibition in alternative or terminal pathway assays. Novel anti-CSMD1 monoclonal antibodies cross-reactive with human and mouse CSMD1 were generated that detected endogenous CSMD1 in human and rodent brain; immunostaining showed predominantly astrocyte and synaptic localisation of CSMD1, the latter confirmed using isolated synapses. Using iPSC-derived cells, astrocyte expression was confirmed and expression on cortical neurons demonstrated. We show that CSMD1 is a classical pathway-specific complement regulator expressed predominantly on astrocytes, neurons, and synapses in human and mouse brain. These findings will help reveal the mechanism by which CSMD1 impacts schizophrenia risk.

1. Introduction

The complement system fulfils a critical role in innate immunity, acting rapidly to defend the host organism from invading pathogens and foreign antigens. Complement cytolytic and pro-phagocytic mechanisms are indiscriminate and its pro-inflammatory effects can inflict damage to the host; hence, complement is tightly regulated at many points in the cascade by numerous membrane-bound and soluble regulatory proteins (Schmidt et al., 2016). Over the past two decades, a complex role of complement has been described in the central nervous system (CNS). Knockout (KO) of classical pathway genes *C1qa*, *C3* or *C4* resulted in aberrant developmental synaptic pruning in mice, implicating complement in brain development (Stevens et al., 2007; Schafer et al., 2012; Sekar et al., 2016). In mouse models of Alzheimer's disease (AD), blocking of classical pathway activation via KO of *C1qa* or *C3* or terminal pathway blockade by KO of *C6* or *C7* or treatment with a C7-blocking antibody, ameliorated synapse loss (Hong et al., 2016; Shi et al., 2017; Wu et al., 2019; Carpanini et al., 2022; Zelek et al., 2024a; b). These findings demonstrate that complement plays a key role in both developmental and pathological synapse loss in mice. In humans,

* Corresponding author at: UK Dementia Research Institute, School of Medicine, Cardiff University, Hadyn Ellis Building, Maindy Road, Cardiff, Wales CF24 4HQ, UK.
** Corresponding author at: UK Dementia Research Institute, School of Medicine, Cardiff University, Hadyn Ellis Building, Maindy Road, Cardiff, Wales CF24 4HQ, UK.
E-mail addresses: ByrneR8@cardiff.ac.uk (R.A.J. Byrne), MorganBP@cardiff.ac.uk (B.P. Morgan).

https://doi.org/10.1016/j.bbi.2025.03.026
Received 8 November 2024; Received in revised form 16 March 2025; Accepted 17 March 2025
Available online 18 March 2025

altered synaptic pruning has long been postulated to contribute to the pathophysiology of schizophrenia (Feinberg, 1982). Recent studies have implicated complement in this process; common complex variation at the complement *C4* locus associated with increased expression of complement C4A was identified as a risk factor for schizophrenia, possibly mediated by dysregulated complement-mediated synaptic pruning (Sekar et al., 2016; Sellgren et al., 2019; Comer et al., 2020; Yilmaz et al., 2021).

Genome-wide association studies (GWAS) of schizophrenia have robustly identified risk variants in the vicinity of *CSMD1*, encoding a putative novel complement regulator (Trubetskoy et al., 2022). *CSMD1* encodes a 388 kDa (3564 amino acid) transmembrane protein comprising 14 N-terminal C1r/s, uEGF and BMP1 (CUB) domains, each separated from the adjacent CUB module by a single short consensus repeat (SCR) domain, followed by 15 tandem C-terminal SCR domains (Kraus et al., 2006). *CSMD1* is primarily expressed in brain and reproductive tissues in humans, rats, and mice (Kraus et al., 2006; Escudero-Esparza et al., 2013; Steen et al., 2013), and may be involved in a variety of physiological functions including tumour suppression, gonadal development, and brain development (Kraus et al., 2006; Lee et al., 2019; Gialeli et al., 2021). Complement regulation by CSMD1 was first reported in 2006; a recombinant fragment comprising the final two C-terminal SCR-CUB repeats and twelve of the C-terminal tandem SCR domains (SCR14-25) of rat CSMD1 inhibited activation of the classical pathway, but not the alternative pathway (Kraus et al., 2006). A second report demonstrated complement regulation on human CSMD1-expressing cells, and investigated two tandem SCR regions in CSMD1, SCR17-21 and SCR23-26, that displayed high sequence homology with other SCR-containing complement regulators (Escudero-Esparza et al., 2013). CSMD1 SCR17-21 inhibited activation of the classical pathway *in vitro* by acting as a cofactor for cleavage of C3b and C4b by factor I (FI), while SCR23-26 possessed no complement regulatory properties. These authors reported that SCR17-21 additionally inhibited membrane attack complex (MAC) assembly via interaction with C7 and to a lesser extent C8.

Since the publication of these two studies, no further work investigating the complement regulatory activity of CSMD1 has been published. Several questions remain unanswered, including precisely how CSMD1 inhibits the C3 convertase, whether it has convertase decay accelerating activity, and how it inhibits the terminal pathway. This latter property in an SCR-containing protein is unexpected, although others reported that the SCR-containing factor H-related protein 1 (FHR1) impeded MAC assembly by binding to C5b6 (Heinen et al., 2009; Michelfelder et al., 2018). There is also a lack of data on what cell types express CSMD1 in human and mouse brain, largely a consequence of the lack of validated CSMD1 antibodies, with only two published studies reporting neuronal expression of CSMD1 protein in rodent tissue (Baum et al., 2024; Kraus et al., 2006). Although a handful of CSMD1 antibodies, mostly polyclonal (pAbs), have been reported and made available commercially, their specificity and utility in core methods such as enzyme-linked immunosorbent assay (ELISA) and immunohistochemistry (IHC) is not clear, an issue that impacts study of the link between complement and schizophrenia (Sekar et al., 2016; Sellgren et al., 2019; Comer et al., 2020).

The dearth of studies and residual uncertainties necessitate replication and further characterisation of the complement inhibiting properties of CSMD1 and its potential role in regulation of complement in the brain. To address these gaps, we recombinantly expressed CSMD1 regions SCR17-21 and SCR23-26 as Fc-fusion proteins and characterised their complement regulatory properties via an array of functional assays. Additionally, we generated a panel of mouse monoclonal antibodies (mAbs) against CSMD1 SCR17-21 that detect intact human and mouse CSMD1 in cells and tissues and utilised them to investigate which brain cell types express CSMD1 in these species.

2. Materials and methods

2.1. Chemicals

Reagents and chemicals were of analytical grade and were purchased from Fisher Scientific unless stated otherwise. Composition of phosphate-buffered saline (PBS) is 137 mM NaCl, 2.7 mM KCl, 10 mM Na_2HPO_4, 1.8 mM KH_2PO_4, pH 7.4. HEPES-buffered saline (HBS) comprises 10 mM HEPES, 150 mM NaCl, 135 μM $CaCl_2$, 1 mM $MgCl_2$, pH 7.4. Alternative pathway buffer (APB) comprises 10 mM HEPES, 150 mM NaCl, 3 mM $MgCl_2$, 5 mM EGTA, pH 7.4. Borate-buffered saline (BBS) composition is 100 mM H_3BO_3, 75 mM NaCl, 25 mM $Na_2B_4O_7$, pH 8.0.

2.2. Cell culture

SP2/0-Ag14 mouse myeloma cells (European Collection of Animal Cell Cultures) were cultured in RPMI 1640 medium containing 2 % (w/v) penicillin/streptomycin, 2 mM glutamine, 1 mM sodium pyruvate, and 15 % (v/v) foetal bovine serum (FBS; Gibco) at 37 °C (5 % CO_2). Expi293F cells (Gibco) were cultured in Expi293F medium (37 °C, 8 % CO_2). KOLF2 induced pluripotent stem cells (iPSCs; Wellcome Trust Sanger Institute) were cultured in mTeSR Plus medium (STEMCELL Technologies) at 37 °C (5 % CO_2) on plates coated with Geltrex (Thermo Fisher Scientific, A1413201). Published methods were followed for differentiation of iPSCs into cortical neurons and astrocytes (Shi et al., 2012; Serio et al., 2013; Maguire et al., 2021).

2.3. Animals

All animal procedures performed were compliant with the Animals Scientific Procedures Act 1986 and local institutional regulations. C57BL/6 wild-type (WT) mice (Envigo) were group-housed in environmentally enriched cages, under standard pathogen-free conditions, with a 12-hour light/dark cycle, food, and water available *ad libitum*. Mice were humanely sacrificed via asphyxiation with increasing CO_2 concentration, death was confirmed by palpation. Whole blood was collected by transcardial puncture, incubated at room temperature (RT; 10 min) to allow clotting, followed by 1 h on ice, and then centrifuged at 17,000 x *g* (15 min, 4 °C). Serum was removed and stored at −80 °C. Exsanguinated mice were intracardially perfused with cold PBS, brains were extracted and halved sagittally, one half stored in 1.5 % (w/v) paraformaldehyde (PFA) for use in immunofluorescence, the other half snap frozen in liquid nitrogen and stored at −80 °C for synaptoneurosome isolation performed as described previously (Carpanini et al., 2022).

2.4. Human tissue

Cryopreserved post-mortem brain tissue from five AD cases (Braak VI) and five controls was provided by the Edinburgh Brain Bank (Table S1). Immunostaining was performed on AD tissue; synaptoneurosomes were isolated from control tissue using published methods (Tzioras et al., 2023). Use of human tissue for post-mortem studies was reviewed and approved by the Edinburgh Brain Bank Ethics Committee and the Medical Research Ethics Committee (the Academic and Clinical Central Office for Research and Development, a joint office of the University of Edinburgh and NHS Lothian, approval number 15-HV-016). The Edinburgh Brain Bank is a Medical Research Council funded facility with Research Ethics Committee (REC) approval (16/ES/0084).

2.5. Protein expression and purification

Custom pcDNA3.1 plasmids encoding human CSMD1 SCR17-21 and SCR23-26 with C-terminal human IgG3-Fc-tags were designed in-house and purchased from GenScript. Plasmid stocks were established by transformation of DH5α *Escherichia coli* (Invitrogen), inoculation of

overnight culture, and plasmid isolation via maxi-prep (QIAGEN; manufacturer's instructions). CSMD1 Fc-fusion proteins were expressed by transfection of Expi293F cells according to the manufacturer's instructions (Thermo Fisher Scientific); purification was performed using protein G affinity with a 5 ml HiTrap Protein G HP column (Cytiva; manufacturer's instructions) followed by overnight dialysis (4 °C) into PBS with 12–14 kDa cut-off dialysis tubing (Medicell). Aggregates were removed and pure CSMD1 Fc-fusion proteins desalted into HBS by size-exclusion chromatography on a Superdex 200 column (Cytiva; manufacturer's instructions). Protein concentrations were determined by BCA assay (Thermo Fisher Scientific; manufacturer's instructions).

2.6. Haemolytic assays

Antibody-sensitised sheep erythrocytes (ShEA) were generated by isolating erythrocytes from blood (TCS Biosciences) and sensitising with Amboceptor (Siemens) as described previously (Zelek et al., 2019; Zelek and Morgan, 2020; Byrne et al., 2021). Rabbit erythrocytes (RbE) were prepared from blood (TCS Biosciences) as described (Zelek et al., 2019). HBS containing calcium and/or magnesium ions was used in haemolysis assays as described (Zelek et al., 2018a). Classical pathway regulatory properties of CSMD1 Fc-fusion proteins, the positive control APT070 comprising SCR1-3 of human complement receptor 1 (CR1; gifted by Dr. Richard Smith, King's College London), and the negative control polyclonal human IgG3 (in-house) were investigated as follows: ShEA were diluted to 2 % (v/v) in HBS and added (50 μl/well) to a serial dilution of each test protein in HBS (100–0 μg/ml; 50 μl/well) in a 96-well round-bottom plate; all wells were supplemented with a dose of normal human serum (NHS; 2.5 % in HBS) previously calculated to give near-complete lysis. ShEA (50 μl/well) supplemented with 100 μl/well of HBS or ddH_2O were used as references for 0 % and 100 % lysis, respectively. Plates were incubated at 37 °C (30 min), centrifuged at 800 x *g* (5 min, 4 °C), supernatant (100 μl/well) transferred to a 96-well flat-bottom plate and absorbance at 405 nm measured with a FLUOstar™ Omega Microplate Reader (BMG LABTECH). Alternative pathway regulatory activity was investigated as above with 2 % RbE instead of 2 % ShEA, APB instead of HBS (containing EGTA to inhibit classical pathway activation), and 25 % NHS instead of 2.5 % NHS.

Decay acceleration and inhibition of classical pathway convertase assembly by CSMD1 Fc-fusion proteins was assessed as follows: C5-depleted human serum (C5DHS; in-house; 5 % in HBS; 50 μl/well) was added to ShEA (2 % in HBS; 50 μl/well) in 96-well plates and incubated at 37 °C (10 min) to allow convertase assembly. Inhibition of convertase assembly was tested by including serial dilutions of each test protein in HBS (100–0 μg/ml; 50 μl/well). Plates were centrifuged (800 x *g*, 1 min), supernatant removed, ShEA washed with cold HBS (200 μl/well) and resuspended in 50 μl/well HBS. NHS (2.5 % in HBS containing 40 mM EDTA, 50 μl/well) was added and incubated at 37 °C (30 min) to develop lysis from the residual pre-formed convertases. Convertase decay acceleration was assessed by generating convertase as above, incubating the convertase-coated cells at 37 °C (10 min) with a serial dilution of each test protein in HBS containing 40 mM EDTA (100–0 μg/ml; 50 μl/well), washing and developing lysis as above. In both assays, percentage lysis was measured as for the standard haemolysis assay.

Terminal pathway inhibition by CSMD1 Fc-fusion proteins was investigated using reactive lysis as described (Zelek et al., 2018b; Zelek and Morgan, 2020). Guinea pig erythrocytes (GpE; TCS Biosciences) were diluted to 1 % (v/v) in HBS and aliquoted into a 96-well round-bottom plate (50 μl/well). Terminal pathway components (purified in-house) were sequentially added (each at 12.5 μl/well), each addition separated by a 10-minute incubation at 37 °C; C5b6 (45 ng/ml final concentration in 150 μl), C7 (184 ng/ml final), C8 (168 ng/ml final), and C9 (383 ng/ml final). The plate was then incubated at 37 °C (30 min) and lysis measured as above. MAC inhibition by the test proteins was assessed by adding them in serial dilution in HBS (100–0 μg/ml; 50 μl/well) prior to addition of C7 or by pre-incubating with C7 or C8 (30 min, 37 °C) prior to addition to the cells to replicate a published study (Escudero-Esparza et al., 2013). Plates were centrifuged and haemolysis measured as before.

2.7. Factor I cofactor assays

C3 was purified from human plasma according to published methods (Ruseva and Heurich, 2014); C4 was immunoaffinity purified from human serum using a HiTrap NHS-Activated HP column coupled to the anti-human C4 mAb D5H3 (in-house) according to the manufacturer's instructions (Cytiva). Methylamine-inactivated C3 ($C3_{MA}$) and C4 ($C4_{MA}$) were generated by incubating the respective proteins (0.5 mg/ml) with 0.1 M methylamine (Merck) in BBS at 37 °C (2 h), then dialysed into PBS overnight (4 °C). FI cofactor activity of CSMD1 Fc-fusion proteins was investigated by incubating candidate cofactors (100 μg/ml) with $C3_{MA}$ or $C4_{MA}$ (50 μg/ml) and FI (10 μg/ml; in-house) in HBS overnight at 37 °C. Reactions were stopped by adding reducing sample buffer and analysed via western blot (see SDS-PAGE).

2.8. Antibody Generation

WT mice (8–16 weeks of age) were immunised subcutaneously with CSMD1 SCR17-21-Fc (50 μg) emulsified in complete Freund's adjuvant (Thermo Fisher Scientific). Mice were boosted with CSMD1 SCR17-21-Fc (50 μg delivered subcutaneously in incomplete Freund's adjuvant; Thermo Fisher Scientific) four and five weeks after initial immunisation, tail-bled one week after the second boost, and serum tested for immunoreactivity against CSMD1 SCR17-21-Fc via ELISA with the antigen immobilised on the wells. Mice with the strongest immune responses were boosted intra-peritoneally with CSMD1 SCR17-21-Fc (50 μg in PBS), humanely killed and splenectomised two days later. Splenocytes were harvested and fused with SP2/0-Ag14 cells; hybridomas were selected using an established protocol (Zelek et al., 2019; Zelek and Morgan, 2020; Byrne et al., 2021). Two weeks after fusion, conditioned medium was harvested from each well and screened for immunoreactivity against CSMD1 SCR17-21 by ELISA. Positive clones were subcloned via limiting dilution three times to ensure monoclonality. Selected CSMD1 SCR17-21-specific monoclonal hybridomas were expanded, isotyped with an IsoStrip™ Mouse Monoclonal Antibody Isotyping Kit (Roche), then inoculated into CELLine™ 1000 bioreactor flasks (Corning). Conditioned media were harvested every 7–10 days and IgG mAbs purified via protein G affinity chromatography. Selected mAbs were conjugated to EZ-Link Sulfo-NHS-LC-Biotin according to the manufacturer's instructions (Thermo Fisher Scientific).

2.9. CSMD1 sandwich ELISA

CSMD1 Fc-fusion proteins were reduced to monomers with 5 mM TCEP and alkylated with 18.75 mM iodoacetamide according to the manufacturer's instructions (Thermo Fisher Scientific). The mAb 3D10 was diluted to 5 μg/ml in carbonate buffer (35 mM $NaHCO_3$, 15 mM Na_2CO_3, pH 9.6), dispensed (50 μl/well) into Nunc MaxiSorp™ flat-bottom 96-well plates (Invitrogen), and incubated overnight (4 °C). Blocking was performed with 100 μl/well 2 % (w/v) bovine serum albumin (BSA) in PBS with 0.05 % (w/v) Tween-20 (PBS-T) for 1 h (37 °C). Wells were washed three times with PBS-T (300 μl/well), and either CSMD1 Fc-fusion protein monomers (1.25 μg/ml), neat NHS, neat cerebrospinal fluid (CSF) or mouse brain homogenate (2.5 mg/ml) were titrated in 0.2 % (w/v) BSA-PBS-T (50 μl/well) and incubated for 90 min (37 °C). Wells were washed as above then incubated with a 2 μg/ml dilution (50 μl/well) of biotinylated mAb 10A5 for 1 h (37 °C). Wells were washed again and incubated with a 1:200 dilution (50 μl/well) of peroxidase-conjugated streptavidin (R&D Systems) for 1 h (37 °C). A final wash was performed, followed by development with O-phenylenediamine dihydrochloride (SIGMAFAST™ OPD, SigmaAldrich). Absorbance was measured at 492 nm with a FLUOstar™ Omega

Microplate Reader.

2.10. SDS-PAGE

Samples were diluted with 5x SDS sample buffer (250 mM Tris-HCl, pH 6.8; 50 % (v/v) glycerol, 5 % (w/v) SDS, 0.1 % (w/v) bromophenol blue) with or without 5 % (v/v) ß-mercaptoethanol and heated at 95 °C (5 min). Samples were resolved on mPAGE 4–12 % Bis-Tris polyacrylamide gels (Bio-Rad) or NuPAGE 3–8 % Tris-acetate polyacrylamide gels with 10–250 kDa PageRuler Plus or 30–460 kDa HiMark pre-stained protein standards, respectively (all from Thermo Fisher Scientific). For protein staining, gels were incubated in InstantBlue Coomassie Protein Stain according to the manufacturer's instructions (Abcam). For western blotting, proteins were transferred onto Amersham Protran 0.45 Nitrocellulose blotting membrane (Cytiva). For total protein quantification, post-transfer membranes were incubated in Ponceau S staining solution (Thermo Fisher Scientific) and imaged via autoexposure (G:BOX Chemi XX6; Syngene); densitometry was performed using ImageJ (National Institutes of Health). Membranes were blocked in PBS-T containing 5 % (w/v) BSA for 1 h (RT). Membranes were then incubated with antibodies against CSMD1 (2 μg/ml; Abcam, ab166908; or in-house), PSD-95 (1:500; Cell Signalling Technologies, 3450S), synaptophysin (1:500; Abcam, ab32127), histone H3 (1:1,000; Abcam, ab1791), C3b (2 μg/ml; C3.30, in-house), or C4 (2 μg/ml; E8, in-house) in PBS-T with 5 % BSA overnight (4 °C). Membranes were washed with PBS-T and incubated with peroxidase-conjugated donkey anti-mouse IgG or donkey anti-rabbit IgG secondary antibodies (Jackson lmmunoresearch; 715-035-151, 715-035-152) in PBS-T with 5 % BSA for 1 h (RT). Membranes were washed again, developed using Amersham enhanced chemiluminescence (Cytiva), and imaged as above.

2.11. Immunostaining

Mouse brain halves were post-fixed overnight in 1.5 % PFA, transferred to PBS, then cut into 80 μm free-floating coronal sections using a VT1200S vibratome (Leica Biosystems). For mild antigen retrieval, brain sections were transferred to 48-well plates containing citrate buffer (10 mM citric acid, 2 mM EDTA, 0.05 % (v/v) Tween-20, pH 6) and heated at 62 °C (1 h). Some anti-CSMD1 mAbs (5G11, 9F10, 10D9) required stronger antigen retrieval, in which case brain sections were transferred to eppendorfs containing citrate buffer and heated at 95 °C (10 mins). Sections were then blocked and permeabilised in PBS containing 0.1 % (v/v) Triton X-100 (TxPBS) with 5 % (v/v) normal goat serum (NGS; Vector Labs, S-1000) for 1 h (RT). Sections were then incubated with mouse anti-CSMD1 mAbs 3D10, biotinylated 3D10, 5G11, 9F10, or 10D9 (all at 10 μg/ml; in-house), rabbit anti-CSMD1 pAb (1:1,000; Invitrogen, PA5-67358), rabbit anti-GFAP pAb (1:4,000; Dako, Z0334), rabbit anti-glutamine synthetase pAb (1:1,000; Abcam, ab73593), rabbit anti-Iba1 pAb (1:1,000; Wako, 019–19741), or rabbit anti-HuC/D mAb (1:1,000; Abcam, ab184267) in TxPBS overnight (4 °C). Co-labelling with CSMD1 antibodies and cell markers was performed sequentially to avoid non-specific interactions. Pre-adsorption of 3D10 was performed by incubation with a five-fold molar excess of CSMD1 SCR17-21-hIgG3-Fc for three hours (RT), centrifugation at 17,000 x *g* (10 min, RT), then adding supernatant to sections. Pre-adsorption of 10D9 was performed with an excess of CSMD1 SCR17-21-hIgG3-Fc as above. Isotype controls for CSMD1/GFAP co-staining included mouse mAb IgG2b (BioLegend, 400301) and rabbit pAb IgG (Thermo Fisher Scientific, 02–6102). Sections were washed three times with TxPBS and incubated with DAPI (1:1,000; Merck), Alexa Fluor 488-conjugated goat anti-mouse IgG (1:1,000; Invitrogen, A11001), and Alexa Fluor 594-conjugated goat anti-rabbit IgG (1:1,000; Invitrogen, A32740) secondary antibodies in TxPBS for 1 h (RT). Alexa Fluor 488-conjugated streptavidin (1:1,000; Invitrogen, S11223) was used to detect biotinylated 3D10. Sections were washed three times and endogenous autofluorescence quenched with 0.1 % (w/v) Sudan Black B (Alfa Aesar) in 70 % (v/v) ethanol for 10 min (RT), then washed, mounted in FluorSave (Millipore, 345789), and imaged using an SP8 Lightning confocal microscope (Leica Biosystems). To confirm synaptic staining of CSMD1, brain sections were incubated with 3D10 or 10D9 (10 μg/ml), chicken anti-Homer1 pAb (1:1,000; post-synaptic maker; Synaptic Systems, 160006), and guinea pig anti-Bassoon mAb (1:1,000; pre-synaptic marker; Synaptic Systems, 141318) in TxPBS overnight (4 °C). Sections were washed three times and incubated with Alexa Fluor 488-conjugated goat anti-mouse IgG (1:1,000), Alexa Fluor 594-conjugated goat anti-guinea pig IgG (1:1,000; Invitrogen, A11076), and AlexaFluor 647-conjugated anti-chicken IgY (1:1,000; Invitrogen, A21449) secondary antibodies in TxPBS for 1 h (RT). Autofluorescence quenching and imaging were performed as above.

Human primary auditory cortex cryosections (18 μm) were fixed in 4 % PFA for 10 min (RT), then blocked and permeabilised in TxPBS containing 5 % NGS for 1 h (RT). Sections were then incubated with 3D10 anti-CSMD1 (10 μg/ml) and anti-GFAP (1:4,000), anti-Iba1 (1:100), or anti-HuC/D (1:1,000) in TxPBS with 5 % NGS overnight (4 °C). GFAP and 3D10 staining was performed sequentially as for mouse tissue. Sections were washed and incubated with DAPI (1:1,000) or Hoechst 33,342 (1:1,000; Invitrogen), Alexa Fluor 488-conjugated goat anti-rabbit IgG (1:1,000; Invitrogen, A11008), and Alexa Fluor 594-conjugated goat anti-mouse IgG (1:1,000; Invitrogen, A32742) secondary antibodies for 1 h (RT). For co-staining pre-adsorbed 3D10 with anti-GFAP, and for GFAP-positive/CSMD1-positive cell quantification, Alexa Fluor 488-conjugated goat anti-mouse IgG (1:1,000) and Alexa Fluor 594-conjugated goat anti-rabbit IgG (1:1,000) secondary antibodies were used as above. Autofluorescence quenching and imaging were performed as for mouse tissue. To confirm synaptic labelling of CSMD1 in human brain, cryosections were fixed as above and blocked in PBS-T containing 10 % NGS for 1 h (RT). Sections were then incubated with 3D10 anti-CSMD1 (10 μg/ml), anti-Bassoon (1:1,000), and anti-Homer1 (1:1,000) overnight (4 °C). Secondary antibody incubations, autofluorescence quenching, and imaging were performed as for mouse tissue.

iPSC-derived astrocytes and neurons were separately seeded onto sterile glass-bottomed 96-well plates (Greiner) coated with Geltrex (Gibco). Adherent cells were washed with sterile PBS, fixed in 4 % PFA for 10 min (RT), washed three times with PBS-T, and blocked with PBS-T containing 10 % NGS for 30 min (RT). Astrocytes were then incubated with 3D10 anti-CSMD1 (10 μg/ml) and anti-GFAP (1:1,000) in PBS-T with 1 % NGS overnight (4 °C). Neurons were incubated with 3D10 anti-CSMD1 (10 μg/ml) and chicken anti-MAP2 pAb (1:1,000; Abcam, ab92434) as above. All cells were then washed three times. Astrocytes were incubated with Hoechst 33,342 (1:1,000), Alexa Fluor 488-conjugated goat anti-rabbit IgG (1:1,000), and Alexa Fluor 594-conjugated goat anti-mouse IgG (1:1,000) secondary antibodies for 1 h (RT); neurons were incubated with DAPI (1:1,000), Alexa Fluor 488-conjugated goat anti-mouse IgG (1:1,000), and Alexa Fluor 594-conjugated goat anti-chicken IgY (1:1,000; Invitrogen, A32759) secondary antibodies for 1 h (RT). Stained cells were washed three times and imaged as above.

2.12. Image analysis

For quantification of synaptic puncta, four images were taken of stained mouse (n = 6) or human (n = 4) tissue sections on a Leica SP8 confocal microscope (63x objective; image size 184.52 μm^2; single plane). In mouse tissue, the cortical region overlying the hippocampus was quantified. Laser power, gain and detection windows were kept consistent for all images. Images were then cropped into 30 μm^2 regions, imported into Imaris (Version 10, Bitplane, Zurich, Switzerland) and combined into a timeseries. Synapses were isolated in Imaris and classified as excitatory where Homer1 and Bassoon were co-localised. The total number of synapses were considered as the total number of Bassoon-positive puncta, CSMD1-positive synapses were quantified where 3D10 co-localised with Bassoon.

For quantification of CSMD1-positive astrocytes, whole section tile scans were taken on an Axioscan slide Z1 scanner (Zeiss) and imported into QuPath. The total number of GFAP-positive astrocytes and the number of GFAP-positive astrocytes that co-localised with CSMD1 were manually counted and the proportion of CSMD1-positive astrocytes calculated. The proportion of CSMD1-positive astrocytes was quantified in both the grey matter (GM) and white matter (WM) of mouse and human brain sections. In mouse tissue, the GM cortex and WM corpus callosum were quantified overlying the hippocampus.

2.13. Statistical analysis

All statistical analyses were performed with Prism (GraphPad, version 10.4.1). Unpaired *t*-tests were used to compare haemolytic assay IC_{50} values and FI cofactor activity. Paired *t*-tests were used to analyse proportions of CSMD1-positive astrocytes in WM and GM, proportions of CSMD1-positive total synapses and excitatory synapses, and CSMD1 expression levels in total brain homogenate and synaptoneurosomes from the same brain samples. Results are indicated on graphs as * = $p < 0.05$, ** = $p < 0.01$, *** = $p < 0.001$. Figure legends contain statistical information for each experiment and graph, including statistical tests performed, definition of n (number of animals, samples), and definition of error bars (e.g. standard error).

3. Results

3.1. Expression and characterisation of convertase inhibition by CSMD1 SCR domains

Custom pcDNA3.1 plasmids encoding human CSMD1 domains SCR17-21 and SCR23-26 with C-terminal IgG3-Fc-tags were generated (Fig. 1a,b, Fig. S1). Human (h)IgG3-Fc-tags were selected as the extended hinge domain reduces risk of steric inhibition of the CSMD1 domains (Harris et al., 2002a). CSMD1 SCR17-21-hIgG3-Fc and SCR23-26-hIgG3-Fc were expressed in Expi293F cells, purified by protein G affinity chromatography, and polished using size-exclusion chromatography (Fig. 1c).

Complement inhibitory properties of CSMD1 hIgG3-Fc-fusion proteins were tested in classical pathway haemolytic assays; APT070, a molecule comprising SCR1-3 of human CR1 (Smith et al., 2001), and polyclonal hIgG3 were used as positive and negative controls, respectively. Titration of CSMD1 SCR17-21-hIgG3-Fc and SCR23-26-hIgG3-Fc (100–0.2 μg/ml) demonstrated that both Fc-tagged CSMD1 domains efficiently inhibited the classical complement activation pathway; SCR23-26-hIgG3-Fc was twice as potent as SCR17-21-hIgG3-Fc at equimolar doses ($P = 0.018$; Fig. 2a,b). In alternative pathway haemolytic assays, neither CSMD1 SCR17-21-hIgG3-Fc nor SCR23-26-hIgG3-Fc (100–0.2 μg/ml) caused inhibition of lysis (Fig. 2c).

The mode of classical pathway convertase inhibition by CSMD1 hIgG3-Fc-fusion proteins was investigated using assays of convertase assembly and decay and FI cofactor activity. Both CSMD1 domains inhibited classical pathway convertase assembly with comparable efficacy (Fig. 2d,e). When tested in assays of classical convertase decay, while the positive control APT070 caused accelerated decay, neither of the CSMD1 domains impacted rate of decay (Fig. 2f). Both SCR17-21-hIgG3-Fc and SCR23-26-hIgG3-Fc enhanced cleavage of $C4_{MA}$, evidenced by increased abundance of the C4d fragment and significantly increased C4d:C4α/α' ratio compared to the hIgG3 negative control ($P < 0.05$; Fig. 2g,h). In contrast, neither CSMD1 domain caused enhanced cleavage of $C3_{MA}$ in FI cofactor assays (Fig. 2i), confirming classical convertase specificity.

3.2. Testing impact of CSMD1 SCR domains on the terminal pathway

The CSMD1 SCR17-21 domain was reported to additionally inhibit the terminal complement pathway (Escudero-Esparza et al., 2013); to test this surprising finding we performed reactive lysis assays. Recombinant soluble (s)CD59 N18Q, a non-N-glycosylated form of CD59 with comparable activity to glycosylated sCD59 (Bodian et al., 1997), was used as a positive control. MAC was assembled *in vitro* on GpE via reactive lysis by sequential incubation with C5b6, C7, C8, and C9; omission of any one of these terminal components abolished lysis and

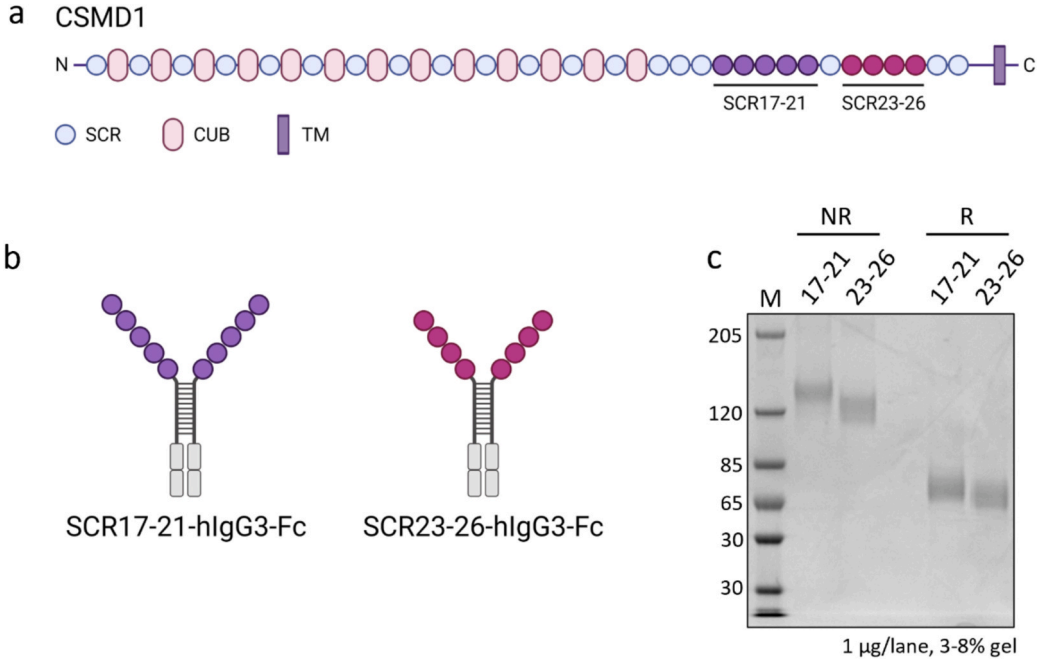

Fig. 1. CSMD1 structure and expression of putative complement regulatory domains. (**a**) CSMD1 structure with the putative complement regulatory regions, SCR17-21 and SCR23-26, highlighted (CUB, complement C1r/C1s, uEGF, BMP1 domain; SCR, short consensus repeat domain; TM, transmembrane domain). (**b**) Structures of CSMD1 SCR17-21 and SCR23-26 hIgG3-Fc-fusion proteins. (**c**) Coomassie stained SDS-PAGE gel of CSMD1 SCR17-21-hIgG3-Fc and SCR23-26-hIgG3-Fc following size-exclusion chromatography under non-reducing (NR) and reducing (R) conditions. Figures created with BioRender.com.

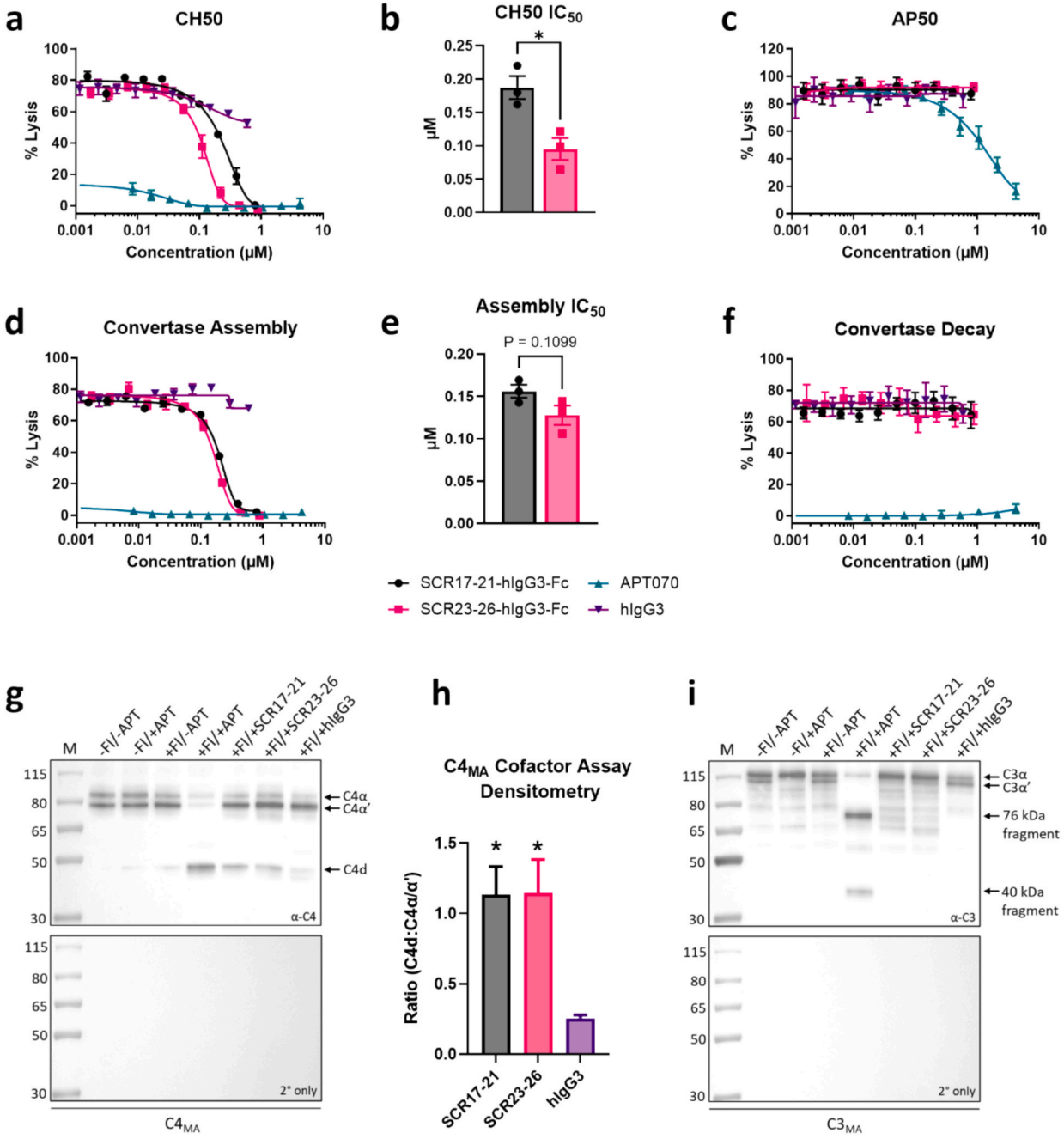

Fig. 2. CSMD1 fusion proteins inhibit the classical pathway through FI cofactor activity. (**a**) Classical pathway haemolytic assay displaying titration of CSMD1 SCR17-21-hIgG3-Fc and SCR23-26-hIgG3-Fc (and APT070 as positive control) with concentrations plotted in μM. (**b**) Calculated IC_{50} doses of CSMD1 fusion proteins interpolated from (**a**). (**c**) Alternative pathway haemolytic assay displaying titration of CSMD1 fusion proteins with concentrations plotted in μM. (**d**) Classical pathway convertase assembly assay displaying titration of CSMD1 fusion proteins with concentrations plotted in μM. (**e**) Calculated IC_{50} of CSMD1 fusion proteins interpolated from (**d**). (**f**) Classical pathway convertase decay assay displaying titration of CSMD1 fusion proteins with concentrations plotted in μM. (**g,i**) Representative western blots of $C4_{MA}$ and $C3_{MA}$ FI cofactor assays (0.5 μg $C4_{MA}$/lane or $C3_{MA}$/lane); CSMD1 fusion proteins increased FI-mediated cleavage of $C4_{MA}$ but not $C3_{MA}$. FI cofactor assays were performed three times with comparable results. (**h**) Densitometry of three independent $C4_{MA}$ FI cofactor assays; C4d band intensity was quantified relative to C4α/α' within each lane. Uncropped westerns are shown in Fig. S2. Unpaired *t*-tests were used to analyse differences between SCR17-21-hIgG3-Fc and SCR23-26-hIgG3-Fc in (**b**) and (**e**), and to compare hIgG3 with each CSMD1 fragment in (**h**). All error bars represent standard error of three independent experiments performed in duplicate except for (**h**), which was three independent experiments without replicates; * = $P < 0.05$.

inclusion of sCD59 N18Q (100 μg/ml) caused complete inhibition (Fig. 3a). Addition of CSMD1 SCR17-21-hIgG3-Fc or SCR23-26-hIgG3-Fc (100–0.2 μg/ml) to C5b6-coated GpE prior to supplementation with C7 did not inhibit lysis, demonstrating that neither domain caused terminal pathway inhibition downstream of C5b6 (Fig. 3b). The published study reported inhibition when CSMD1 SCR17-21 was pre-incubated with C7 or C8 (Escudero-Esparza et al., 2013). To test this, CSMD1 domains (100–0.2 μg/ml) were preincubated with C7 prior to addition to C5b6-coated GpE or C8 prior to addition to C5b67-coated GpE; neither of these pre-treatments resulted in inhibition of lysis when the respective CSMD1 domains preincubated with C7 or C8 were added into the reactive lysis system (Fig. 3c,d). These data demonstrate that CSMD1 SCR domains do not inhibit terminal pathway activity and MAC assembly.

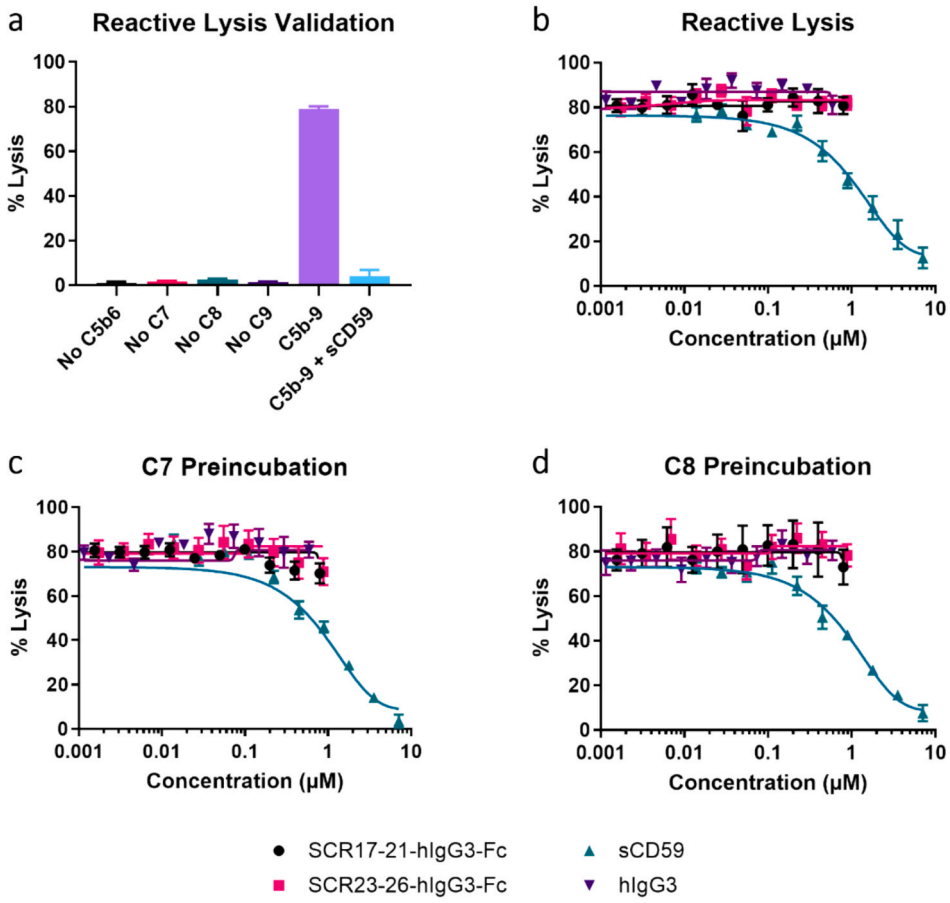

Fig. 3. CSMD1 fusion proteins do not inhibit the terminal pathway. (**a**) Reactive lysis assay validation. C5b6, C7, C8, and C9 were added sequentially to guinea pig erythrocytes to cause MAC assembly and lysis. All components were essential for lysis, inclusion of sCD59 N18Q inhibited lysis. (**b**) Titration of CSMD1 SCR17-21-hIgG3-Fc and SCR23-26-hIgG3-Fc added to GpE-C5b6 prior to addition of C7; sCD59 was titrated as positive control. (**c**) C7 pre-incubated (30 min at 37 °C) with CSMD1 fusion proteins prior to addition to GpE-C5b6 as above. (**d**) C8 pre-incubated with CSMD1 fusion proteins prior to addition to GpE-C5b6 as above. The fusion proteins showed no inhibition in any of the assays. Error bars in (**a**) represent standard error of triplicates from one experiment. Error bars in (**b**), (**c**), and (**d**) represent standard error of three independent experiments performed in duplicate. All test proteins were titrated from 100–0.2 μg/ml and data plotted in μM.

3.3. Generation and characterisation of CSMD1 antibodies

CSMD1 SCR17-21-hIgG3-Fc-immunised mice with the highest specific antibody titre were identified via ELISA (Fig. S3a), hybridomas were generated and screened against CSMD1 SCR17-21-hIgG3-Fc and human IgG; clones that also reacted with human IgG were discarded as likely Fc-reactive (Fig. S3b,c). Six clones producing IgG mAbs specific to CSMD1 SCR17-21 were identified, expanded and mAbs purified via protein G affinity chromatography (Fig. S3d). The mAbs were all either IgG2b (3D10, 10A5, 10D9) or IgG1 (3H3, 5G11, 9F10). Specificity to CSMD1 SCR17-21 over CSMD1 SCR23-26 was confirmed by direct ELISA (Fig. 4a). A sandwich ELISA comprising 3D10 capture and biotinylated 10A5 detection showed dose-dependent measurement of monomeric SCR17-21-hIgG3-Fc down to 10 ng/ml; the assay detected CSMD1 in mouse brain homogenate, but did not detect any soluble CSMD1 in human serum or CSF (Fig. 4b). Five of the six selected mAbs recognised endogenous mouse and human CSMD1 as a ~ 388 kDa doublet in western blots of brain homogenates (Fig. 4c). The mAb 3D10 showed negligible signal in western blots but was retained because it displayed good signal in ELISA and immunostaining in mouse and human brain tissue.

3.4. Identification of CSMD1-expressing brain cell types

Free-floating mouse brain sections were co-stained with mAb 3D10 and specific markers for the major brain cell types, neurons (HuC/D), astrocytes (GFAP), and microglia (Iba1). The mAb 3D10 stained cells that also expressed GFAP in the cortex and hippocampus, indicating that 3D10 labelled astrocytes in mouse brain; specificity was confirmed by pre-adsorption of the mAb resulting in loss of 3D10 immunostaining (Fig. 5a,b). Punctate background staining suggestive of synapses was present and abolished by pre-adsorption. 3D10 also labelled glutamine synthetase-expressing astrocytes (Fig. S5a); there was trace staining of HuC/D-expressing neurons, negligible after pre-adsorption of the antibody, and no staining of Iba1-positive microglia (Fig. S5b). Astrocytic and punctate staining were also observed with other in-house anti-CSMD1 mAbs (Fig. S6). No positive staining was observed with a commercial anti-CSMD1 rabbit pAb (Invitrogen, PA5-67358; data not shown). GFAP-positive/CSMD1-positive cells were quantified; the proportion of GFAP-positive cells expressing CSMD1 was significantly enriched in WM relative to GM in mouse brain ($P < 0.001$; Fig. 5c-e).

Human primary auditory cortex tissue sections were co-stained with 3D10 and specific cell markers; as in mouse, 3D10 staining co-localised with GFAP-expressing cells indicating that CSMD1 is expressed on astrocytes (Fig. 6a), with specificity confirmed by pre-adsorption (Fig. S7a). No CSMD1 expression was observed on neurons (HuC/D+) or microglia (Iba1+; Fig. S7b). To verify our findings, human iPSCs were differentiated into astrocytes and cortical neurons then stained with 3D10 and the appropriate cell markers. CSMD1 expression was detected on both GFAP-expressing iPSC-derived astrocytes and MAP2-expressing cortical neurons (Fig. 6b,c). GFAP-positive/CSMD1-positive cells were quantified in the human AD brain; there was no significant difference

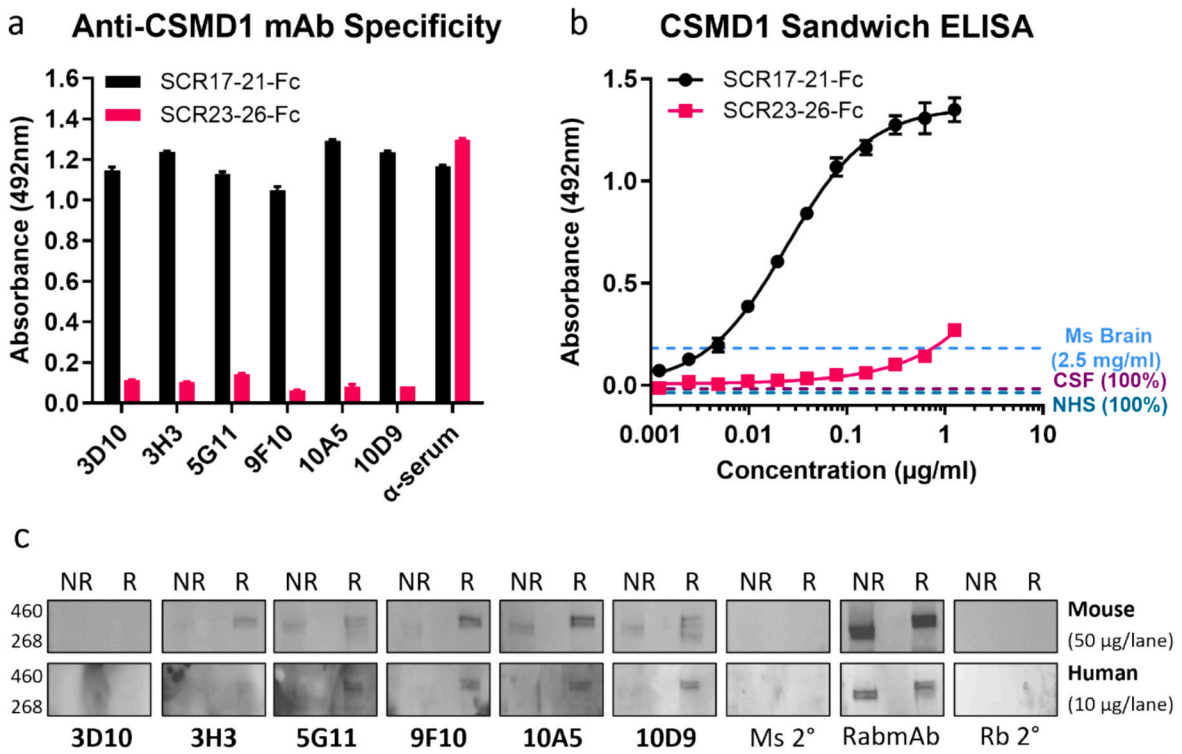

Fig. 4. Characterisation of CSMD1 mAbs. (**a**) Direct ELISA data displaying binding of anti-CSMD1 SCR17-21 mAbs (2 µg/ml) to immobilised CSMD1 SCR17-21-hIgG3-Fc or SCR23-26-hIgG3-Fc (0.5 µg/ml). Mouse immune serum (α-serum) was used as a positive control; error bars are standard error of triplicates. (**b**) CSMD1 sandwich ELISA displaying standard curves of CSMD1 SCR17-21-hIgG3-Fc dilutions with SCR23-26-hIgG3-Fc as a control; absorbance values are indicated on the y-axis for mouse brain homogenate (tested at 2.5 mg/ml), undiluted serum (NHS), and undiluted CSF in the assay. Error bars are standard error of three independent experiments performed in duplicate. (**c**) Western blots displaying binding of anti-CSMD1 SCR17-21 mAbs (2 µg/ml) to CSMD1 in mouse (50 µg/lane) and human (10 µg/lane) brain homogenates. Mouse secondary (Ms 2°) only and rabbit (Rb) 2° only blots are negative controls. CSMD1 is a doublet around 388 kDa that shifts upwards with reduction (R). Uncropped westerns are shown in Fig. S4.

between the proportion of GFAP-positive cells expressing CSMD1 in WM compared to GM (Fig. 6d-f).

To confirm whether CSMD1 was expressed at the synapse as suggested by the mouse immunostaining, human and mouse brain sections were co-stained with anti-CSMD1 and synaptic markers. CSMD1 (3D10 staining) co-localised with Bassoon- and Homer1-positive synapses in both mouse and human brain (Fig. 7a,b), demonstrating the presence of CSMD1 at the synapse. Approximately a quarter of analysed Bassoon-positive synapses were CSMD1-positive; significantly enriched proportions of CSMD1-positive synapses were observed in Bassoon-positive/Homer1-positive excitatory synapses in both mouse ($P < 0.001$; Fig. 7c) and human brain ($P = 0.016$; Fig. 7d). To further validate synaptic CSMD1 expression in mouse and human brain, synaptoneurosomes were isolated, validated via western blot (Fig. S8), and CSMD1 expression analysed by western blot (Fig. 7e,f). CSMD1 expression in synaptoneurosomes was significantly elevated relative to total brain homogenate in both mouse ($P < 0.001$; Fig. 7g) and human brain ($P = 0.008$; Fig. 7h), supporting enrichment of CSMD1 at synapses.

4. Discussion

CSMD1 encodes a membrane-bound protein primarily expressed in brain and reproductive tissues (Kraus et al., 2006; Escudero-Esparza et al., 2013). Numerous functions have been ascribed to CSMD1, although it has been most studied as a candidate tumour suppressor (Li et al., 1994; Scholnick et al., 1996; Bockmühl et al., 2001; Ermis Akyuz and Bell, 2022). The first large schizophrenia GWAS identified variants at the *CSMD1* locus that were associated with increased schizophrenia risk (The Schizophrenia Psychiatric Genome-Wide Association Study (GWAS) Consortium, 2011), suggesting that CSMD1 might have roles in maintaining brain health. Later genetic studies confirmed association between *CSMD1* and schizophrenia (Ripke et al., 2013; Schizophrenia Working Group of the Psychiatric Genomics Consortium, 2014; Pardiñas et al., 2018; Trubetskoy et al., 2022) and also identified the *C4A* locus as a major contributor to schizophrenia risk (Sekar et al., 2016), the latter linking the complement system to schizophrenia.

The first suggestion that CSMD1 might be a complement regulator was made almost 20 years ago (Kraus et al., 2006). These authors expressed the C-terminal region of rat CSMD1, comprised of 15 tandem SCR domains, a structural motif typical of complement C3 fragment receptors and C3 convertase regulators, which inhibited the complement classical pathway. These findings were later replicated for human CSMD1; two regions of the C-terminus of CSMD1, SCR17-21 and SCR23-26, were expressed and complement regulatory activity localised to SCR17-21 (Escudero-Esparza et al., 2013). This construct not only inhibited the classical pathway convertase but also inhibited the terminal pathway and MAC assembly. These descriptions of CSMD1 as a complement regulator have not been replicated, in part because tools available for studying CSMD1 expression and function remain scarce.

Given the strong evidence for genetic association of *CSMD1* with schizophrenia and the abundance of evidence implicating complement dysregulation in synapse loss (Stevens et al., 2007; Schafer et al., 2012; Sekar et al., 2016), it is timely to further investigate the complement regulatory properties and brain cell expression of CSMD1. To test function, we expressed CSMD1 SCR17-21 and SCR23-26 as hIgG3-Fc-fusion proteins. We only examined these regions previously identified as candidate complement regulatory domains; SCR-containing regulatory units require a minimum of three consecutive SCR domains (Ojha et al., 2019), and the tandem region SCR14-28 already contains two candidate regulatory units (SCR17-21 and SCR23-26); hence, it is

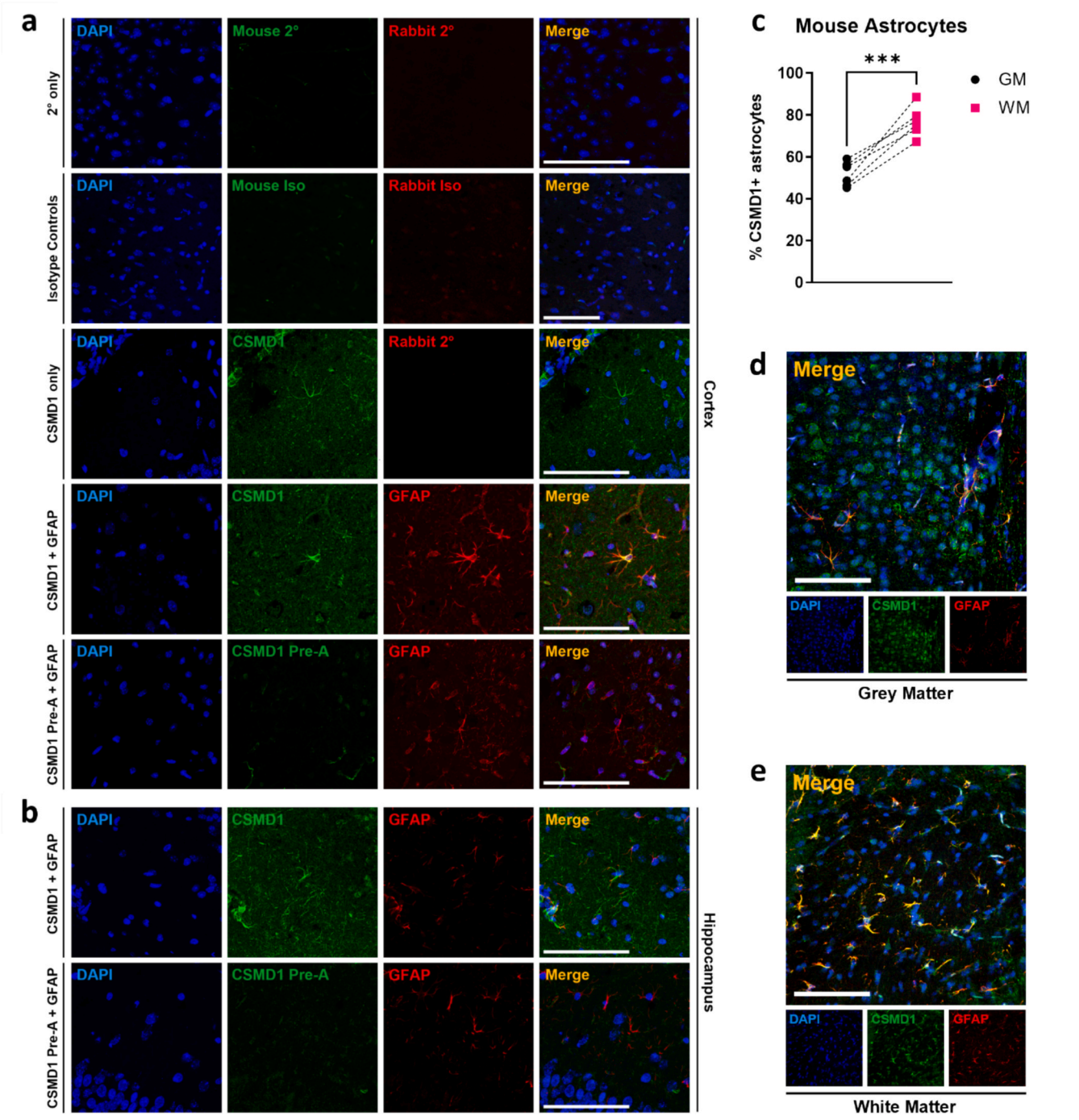

Fig. 5. CSMD1 is expressed by astrocytes in mouse brain. Immunostaining of (**a**) cortex and (**b**) hippocampus of free-floating mouse brain sections with anti-CSMD1 mAb 3D10 (10 μg/ml) co-stained with rabbit anti-GFAP pAb (1:4,000). Controls included mouse IgG2b and rabbit IgG isotype controls (iso; 10 μg/ml), secondary (2°) only controls, and anti-CSMD1 mAb 3D10 pre-adsorbed (Pre-A) with a 5x molar excess of CSMD1 SCR17-21-hIgG3-Fc. Staining in (**a-b**) was performed in duplicate on brain sections from three 6-month-old WT mice. Blood vessel staining by the anti-mouse 2° is visible in the green channel and was not present when biotinylated 3D10 was used (Fig. S5c). (**c**) Quantification of GFAP-positive cells that were CSMD1-positive in GM and WM in 3-month-old WT mice (n = 6). Dashed lines indicate paired data from the same tissue sample; a paired *t*-test was used to calculate significance, *** = P < 0.001. Representative immunostaining of astrocytes in (**d**) grey matter and (**e**) white matter with anti-CSMD1 mAb 3D10 (10 μg/ml) and rabbit anti-GFAP pAb (1:4,000). All images are ~ 15 μm z-stacks. DAPI in the blue channel, anti-mouse-488 to detect the anti-CSMD1 mAb in the green channel, and anti-rabbit-594 to detect the anti-GFAP pAb in the red channel. Scale bars (100 μm) are shown on merged images. (For interpretation of the references to colour in this figure legend, the reader is referred to the web version of this article.)

unlikely that a third regulatory domain exists within SCR14-28.

Both CSMD1 domains efficiently inhibited classical pathway activation in haemolytic assays, in contrast to the previous report that only SCR17-21 displayed complement regulatory activity (Escudero-Esparza et al., 2013). We suggest that this may be due to the use of hIgG1-Fc-tags in their constructs, which we have previously shown cause steric hindrance of fused SCR-containing complement regulator constructs (Harris et al., 2002a; b; 2003). Here we used human IgG3-derived Fc to provide the most flexible hinge region, minimising risk of steric inhibition (Phillips et al., 1994; Harris et al., 2002a). Both of the CSMD1

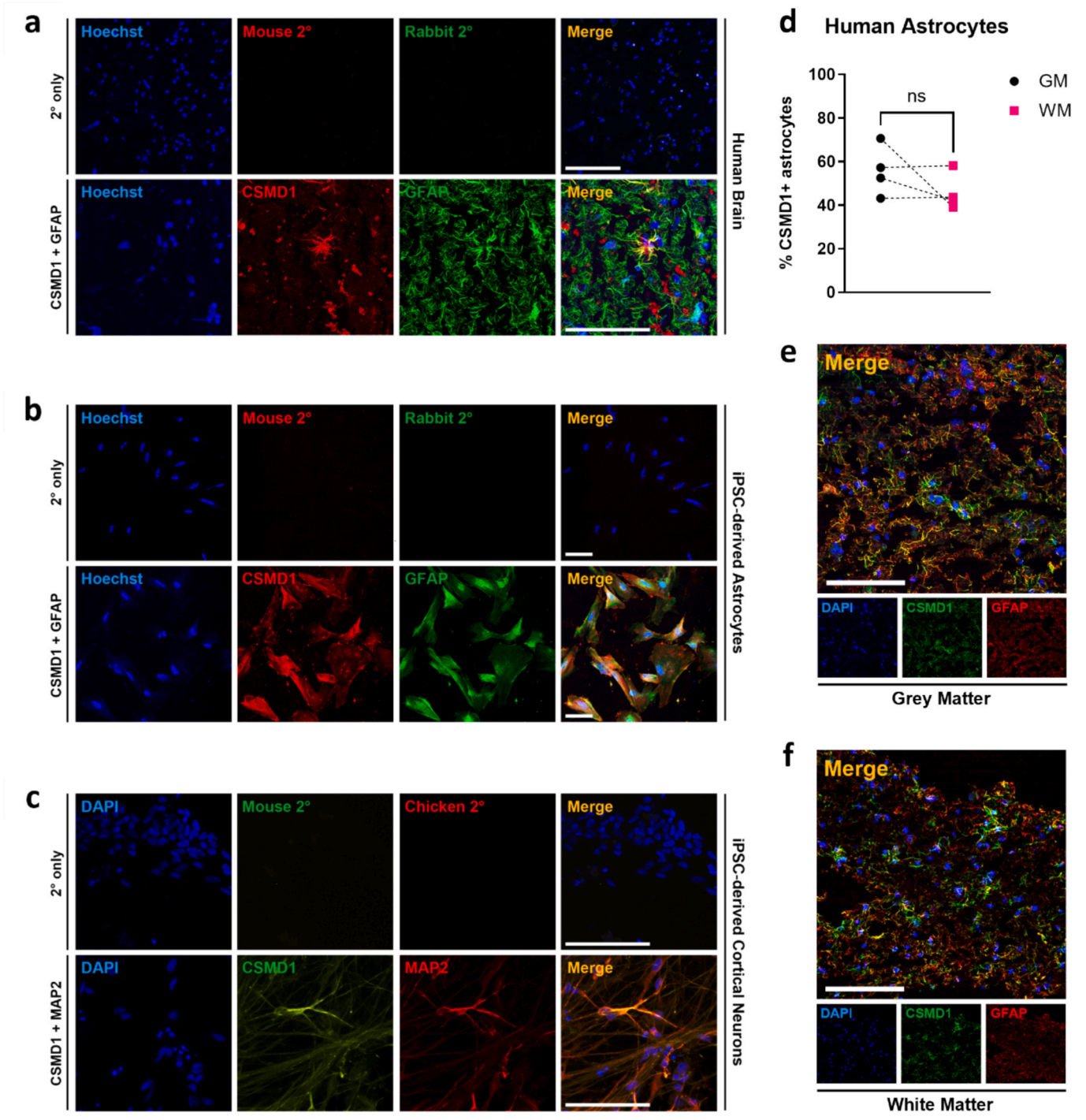

Fig. 6. CSMD1 is expressed by astrocytes in human brain and by iPSC-derived astrocytes and neurons. (**a**) Representative immunostaining of human primary auditory cortex (SD037/18) with anti-CSMD1 mAb 3D10 (10 μg/ml) co-stained with rabbit anti-GFAP pAb (1:4,000). (**b**) Human iPSC-derived astrocytes stained with anti-CSMD1 mAb 3D10 (10 μg/ml) co-stained with rabbit anti-GFAP (1:1,000). In (**a**-**b**), Hoechst is in the blue channel, anti-rabbit-488 to detect the anti-GFAP pAb in the green channel, and anti-mouse-594 to detect the anti-CSMD1 mAb in the red channel. (**c**) Human iPSC-derived cortical neurons immunostained with anti-CSMD1 mAb 3D10 (10 μg/ml), co-stained with chicken anti-MAP2 pAb (1:1,000). DAPI in the blue channel, anti-mouse-488 to detect anti-CSMD1 mAb in the green channel, anti-chicken-594 to detect anti-MAP2 pAb in the red channel. Staining in (**a**-**c**) was performed in duplicate on at least three brain samples or three separate iPSC-derived cell lines; secondary (2°) only controls are included. (**d**) Quantification of GFAP-positive cells that were CSMD1-positive in grey matter (GM) and white matter (WM) in AD cases (n = 4; SD014/19, SD034/17, SD040/18, SD042/17). Dashed lines indicate paired data from the same tissue sample; a paired *t*-test was used to calculate significance. Representative immunostaining of astrocytes in (**e**) GM and (**f**) WM (both in SD042/17) with anti-CSMD1 mAb 3D10 (10 μg/ml) and rabbit anti-GFAP pAb (1:4,000). In (**e**-**f**), DAPI is in the blue channel, anti-mouse-488 to detect the anti-CSMD1 mAb in the green channel, and anti-rabbit-594 to detect the anti-GFAP pAb in the red channel. All images in this figure are ~15 μm z-stacks; scale bars (100 μm) are shown on merged images. (For interpretation of the references to colour in this figure legend, the reader is referred to the web version of this article.)

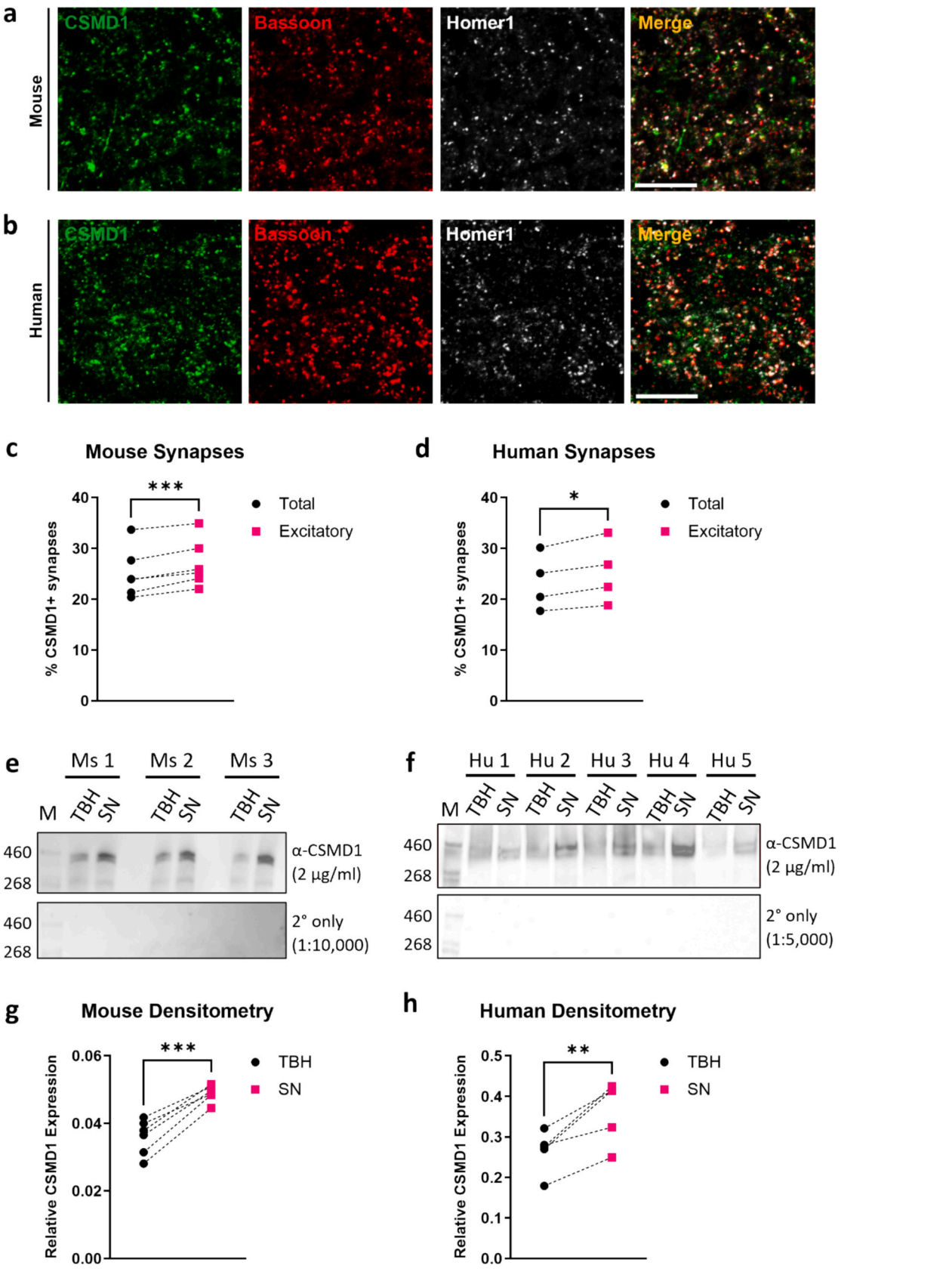

(caption on next page)

Fig. 7. CSMD1 is expressed at synapses in mouse and human brain. Representative immunostaining of (**a**) free-floating mouse brain sections and (**b**) human brain tissue sections with anti-CSMD1 mAb 3D10 (10 μg/ml) co-stained with guinea pig anti-Bassoon mAb (1:1,000) to tag pre-synaptic structures and chicken anti-Homer1 pAb (1:1,000) to tag excitatory synapses. Anti-mouse-488 to detect anti-CSMD1 mAb in the green channel, anti-guinea pig-594 to detect anti-Bassoon mAb in the red channel, anti-chicken-647 to detect anti-Homer1 in the grey channel. Scale bars (10 μm) are on the merged images. Quantification of total synapses (Bassoon-positive) and excitatory synapses (Bassoon-positive/Homer1-positive) that were CSMD1-positive in (**c**) 3-month-old WT mice (n = 6) and (**d**) human AD cases (n = 4; SD014/19, SD034/17, SD040/18, SD042/17). Representative western blots displaying detection of CSMD1 in (**e**) mouse and (**f**) human TBH and SN samples under reducing conditions (50 μg/lane for mouse, 10 μg/lane for human), including secondary (2°) only control. Uncropped westerns are shown in Fig. S9. Western blot densitometry to show CSMD1 signal relative to total protein in TBH and SN samples from (**g**) 4.5-month-old male WT mice (n = 6, no replicates) and (**h**) human controls (n = 5, in duplicate; SD012/17, SD024/17, SD030/18, SD042/18, SD046/17 (Table S1). In all graphs dashed lines indicate paired data from the same tissue sample. Paired *t*-tests were used to calculate significance; * = $P < 0.05$, ** = $P < 0.01$, *** = $P < 0.001$. (For interpretation of the references to colour in this figure legend, the reader is referred to the web version of this article.)

domains inhibited assembly of classical pathway convertases but did not accelerate their decay, suggesting that they acted as FI cofactors. This was tested in cofactor assays using methylamine-inactivated C3 and C4 ($C3_{MA}$, $C4_{MA}$) as substrates for FI cleavage (Nilsson and Nilsson, 1986; Vanderpuye et al., 1994), both CSMD1 domains mediated FI cleavage of $C4_{MA}$ but not $C3_{MA}$, demonstrating specificity for C4 and supporting our haemolysis assay findings showing inhibition of the classical but not alternative pathway. This finding is substantiated by a recent report which utilised co-immunoprecipitation mass spectrometry in mouse forebrain to identify CSMD1-interacting proteins; these included C4b (Baum et al., 2024). These authors also reported an interaction between mouse CSMD1 and C1q, an observation we have not yet investigated. SCR17-21 and SCR23-26 regions are highly conserved between humans and mice (>90 % sequence identity; Fig. S10); however, whether the mouse domains possess comparable complement inhibitory properties remains untested.

The published study reported that CSMD1 SCR17-21 not only inhibited the classical C3 convertase but also blocked the terminal pathway and MAC assembly (Escudero-Esparza et al., 2013). This is a surprising finding given that SCR-containing regulators bind C3 and C4 fragments in the convertases to mediate regulatory activity and no mechanism for interactions with MAC intermediates has been reported. The SCR-containing protein FHR1 was reported to inhibit the terminal pathway but this likely involves interactions with the C5 convertase rather than MAC assembly (Heinen et al., 2009; Michelfelder et al., 2018). To test this reported activity, we used reactive lysis assays where MAC is sequentially assembled from the component proteins on erythrocytes; putative regulators can be added at different stages of MAC assembly (Zelek and Morgan, 2020). Neither CSMD1 SCR17-21 nor CSMD1 SCR23-26 inhibited MAC formation when added at any stage of assembly; in contrast, the terminal pathway regulator sCD59 completely blocked MAC assembly in the assay. Both our study and the published study tested CSMD1 domains at 100 μg/ml; however, the published study utilised a 70 mM NaCl veronal buffer which may permit more non-specific interactions compared to the 150 mM NaCl HBS employed in our assay. To further replicate the published study, the CSMD1 constructs were pre-incubated with C7 or C8 prior to adding into the assay (Escudero-Esparza et al., 2013); again, no inhibition was observed, confirming that the complement regulatory domains in CSMD1 do not regulate MAC assembly.

In order to better assess the distribution of CSMD1 in brain and expression on brain cells we first developed better tools. We generated six mouse mAbs against the CSMD1 SCR17-21 construct; the mAbs were specific for the construct and detected endogenous CSMD1 in western blots of both mouse and human brain homogenates, comparable to a commercial rabbit mAb recommended for use solely in westerns (Abcam, ab166908). To test the existence of a soluble form of CSMD1, we established a sensitive ELISA; the assay detected soluble CSMD1 in brain homogenates but gave no signal in either CSF or plasma. A recent study reported the detection of soluble CSMD1 in plasma with reduced levels in schizophrenia using an unvalidated commercial ELISA; our results do not support this observation (Abd El Gayed et al., 2021). Several of the mAbs worked well in mouse IHC, giving comparable staining patterns. We selected mAb 3D10; this specifically immunostained GFAP- and glutamine synthetase-expressing cells demonstrating that CSMD1 is expressed by astrocytes in both mouse and human brain, an observation that was replicated in iPSC-derived astrocytes. 3D10 signal in brain IHC was eliminated by pre-adsorption of the mAb with the CSMD1 domain, confirming specificity. No CSMD1 signal was detected with a commercial rabbit pAb (PA5-67358, Invitrogen; now discontinued). Astrocytic CSMD1 expression was abundant in the hippocampus and in cortex, notably the prefrontal cortex, a region long-established to be dysfunctional in individuals with schizophrenia (Callicott et al., 2003). We observed a significant enrichment of GFAP-positive cells expressing CSMD1 in GM relative to WM in mouse brain; however, this finding was not replicated in human tissue. This analysis was limited to AD brain tissue; a broader study comparing CSMD1-positive astrocytes in healthy control and AD brain may elucidate whether astrocyte expression of CSMD1 is influenced by astrocyte reactivity in the context of AD. *Csmd1* mRNA expression by mouse astrocytes has previously been reported (Li et al., 2019; Habib et al., 2020; Borgenheimer et al., 2022); however, our data provide the first evidence of CSMD1 protein expression by astrocytes in mouse and human brain.

Neuronal expression of CSMD1 protein has been reported in rodent brain (Kraus et al., 2006; Baum et al., 2024), while several RNA-sequencing studies report substantially higher *CSMD1* expression in neurons compared to astrocytes in both humans and mice (Saunders et al., 2018; Karlsson et al., 2021; Schartz et al., 2024). CSMD1 expression in iPSC-derived glutamatergic cortical neurons has also been reported (Baum et al., 2024), a finding that we replicated in MAP2-expressing iPSC-derived cortical neurons. Although we did not detect CSMD1 expression on neuronal somata by IHC in mouse or human brain, we did observe punctate staining that we confirmed to be synaptic CSMD1 by co-staining with synaptic markers in mice and humans. CSMD1 expression was significantly enriched in both mouse and human synaptoneurosomes, supporting synapse-specific expression of CSMD1, and CSMD1 expression was enriched on Homer1-positive excitatory synapses in both mouse and human brain. Our observations align with a recent study reporting elevated CSMD1 expression in synaptosomes and on VGLUT1/2-positive excitatory synapses in mice (Baum et al., 2024). The precise role of CSMD1 at the synapse remains a matter of conjecture. We suggest that CSMD1 regulates complement classical pathway activation at the synapse, protecting from synapse loss.

The findings from genomic studies implicates dysregulation of the classical complement pathway in the aetiology of the disorder; *CSMD1* and *C4A* are GWAS risk loci and their encoded proteins CSMD1 and C4 converge on the classical pathway, C4 an essential component of the convertase and CSMD1 a key regulator in the brain. Excessive synaptic pruning mediated by dysregulation of the classical pathway has been postulated as one of the pathophysiological mechanisms contributing to schizophrenia, with the role of C4 being extensively studied. Mice expressing human risk variant C4A displayed excessive synaptic pruning during development compared to C4B-expressing mice (Yilmaz et al., 2021), vulnerability of iPSC-derived neurons to C3 fragment deposition increased proportionally with *C4A* copy number (Sellgren et al., 2019), and overexpression of C4 in the mouse prefrontal cortex increased microglial engulfment of synapses (Comer et al., 2020). The authors of the latter study recently suggested that mouse *C4* overexpression-

induced synapse loss may be complement-independent and occur due to impaired AMPAR trafficking, as indicated with *CR3* KO mice and overexpression of C4 mutants that cannot assemble C4b2a (Phadke et al., 2024). However, these findings do not account for phagocytosis mediated by other complement receptors, synaptic engulfment by cells that do not express CR3 such as astrocytes, and the role of alternative pathway convertases that do not include C4b. Together, these data support a scenario where the C4 risk variant enhances complement dysregulation at the synapse to exacerbate synapse loss. In stark contrast, little is known about the roles of CSMD1. One study reported that *CSMD1* KO iPSC-derived glutamatergic cortical neurons were more vulnerable to C3 fragment deposition, *Csmd1* KO mice displayed a reduced number of retinogeniculate synapses and elevated co-localisation of C3 fragments with retinogeniculate synapses, and mouse microglia preferentially engulfed synaptoneurosomes isolated from *Csmd1* KO mice in a complement-dependent manner, all suggesting increased complement activation on neurons and synapses in the absence of CSMD1 (Baum et al., 2024).

Taken together, the data suggest that neuronal-expressed CSMD1 may act to defend neurons from complement deposition and subsequent engulfment of synaptic material by microglia. Hence, we propose that while C4A enhances synaptic pruning, CSMD1, expressed at the synapse and by astrocytes, acts as an inhibitory regulator. A range of astrocyte functions have been suggested to be involved in the aetiology of schizophrenia (Notter, 2021), but understanding of how these could affect schizophrenia pathogenesis and whether CSMD1 plays roles is lacking. Astrocytes contribute to complement-dependant phagocytosis of synapses (Dejanovic et al., 2022); whether schizophrenia risk-associated variants at the *CSMD1* locus cause dysregulation of this process remains unknown. The risk variants in *CSMD1* are non-coding and their impact on expression or function unknown. It may be that these variants cause decreased expression of CSMD1 in the brain, predisposing to complement dysregulation and synapse loss.

In summary, we show that CSMD1 possesses two complement regulatory domains, each with FI cofactor activity specific for the classical pathway convertase. We demonstrate using novel anti-CSMD1 mAbs that CSMD1 is expressed on astrocytes and at synapses in mouse and human brain. The work provides clues to the observed genetic association of CSMD1 with schizophrenia risk and tools for future studies of mechanism.

CRediT authorship contribution statement

Robert A.J. Byrne: Writing – review & editing, Writing – original draft, Methodology, Investigation, Formal analysis, Data curation. **Jacqui Nimmo:** Methodology, Investigation, Formal analysis, Data curation. **Megan Torvell:** Methodology, Investigation, Formal analysis. **Sarah M. Carpanini:** Writing – review & editing, Methodology, Investigation, Formal analysis. **Nikoleta Daskoulidou:** Writing – review & editing, Methodology, Investigation, Formal analysis. **Timothy R. Hughes:** Writing – review & editing, Supervision, Methodology. **Lucy V. Noble:** Validation, Investigation. **Aurora Veteleanu:** Resources, Methodology, Investigation. **Lewis M. Watkins:** Writing – review & editing, Methodology, Investigation. **Wioleta M. Zelek:** Writing – review & editing, Validation, Supervision, Methodology, Investigation, Data curation, Conceptualization. **Michael C. O'Donovan:** Writing – review & editing, Supervision, Data curation, Conceptualization. **Bryan Paul Morgan:** Writing – review & editing, Writing – original draft, Supervision, Resources, Project administration, Funding acquisition, Formal analysis, Data curation, Conceptualization.

Declaration of competing interest

The authors declare the following financial interests/personal relationships which may be considered as potential competing interests: MOD reports receiving grants from the Takeda Pharmaceutical Company Ltd and from Akrivia Health outside the submitted work. Takeda and Akrivia played no part in the conception, design, implementation, or interpretation of this study. The other authors declare that they have no known competing financial interests or personal relationships that could have appeared to influence the work reported in this paper.

Acknowledgements

This work is supported by the Hodge Foundation through a Studentship to RAJB and the UK Dementia Research Institute [award number UK DRI-3002] through UK DRI Ltd, principally funded by the Medical Research Council. The funders were not involved in study design; in the collection, analysis and interpretation of data; in the writing of this report; or in the decision to submit this article for publication. We thank the Edinburgh Brain Bank for providing brain samples, and Dr. Richard Smith for providing APT070.

Appendix A. Supplementary data

Supplementary data to this article can be found online at https://doi.org/10.1016/j.bbi.2025.03.026.

Data availability

The authors confirm that the data supporting the findings of this study are available upon reasonable request.

References

Abd El Gayed, E.M., Rizk, M.S., Ramadan, A.N., Bayomy, N.R., 2021. mRNA expression of the CUB and sushi multiple domains 1 (CSMD1) and its serum protein level as predictors for psychosis in the familial high-risk children and young adults. ACS Omega 6, 24128–24138. https://doi.org/10.1021/acsomega.1c03637.

Baum, M.L., Wilton, D.K., Fox, R.G., Carey, A., Hsu, Y.-H.-H., Hu, R., Jäntti, H.J., Fahey, J.B., Muthukumar, A.K., Salla, N., Crotty, W., Scott-Hewitt, N., Bien, E., Sabatini, D.A., Lanser, T.B., Frouin, A., Gergits, F., Håvik, B., Gialeli, C., Nacu, E., Lage, K., Blom, A.M., Eggan, K., McCarroll, S.A., Johnson, M.B., Stevens, B., 2024. CSMD1 regulates brain complement activity and circuit development. Brain Behav. Immun. 119, 317–332. https://doi.org/10.1016/j.bbi.2024.03.041.

Bockmühl, U., Ishwad, C.S., Ferrell, R.E., Gollin, S.M., 2001. Association of 8p23 deletions with poor survival in head and neck cancer. Otolaryngol. Head Neck Surg. 124, 451–455. https://doi.org/10.1067/mhn.2001.114794.

Bodian, D.L., Davis, S.J., Morgan, B.P., Rushmere, N.K., 1997. Mutational analysis of the active site and antibody epitopes of the complement-inhibitory glycoprotein, CD59. J. Exp. Med. 185, 507–516. https://doi.org/10.1084/jem.185.3.507.

Borgenheimer, E., Hamel, K., Sheeler, C., Moncada, F.L., Sbrocco, K., Zhang, Y., Cvetanovic, M., 2022. Single nuclei RNA sequencing investigation of the Purkinje cell and glial changes in the cerebellum of transgenic Spinocerebellar ataxia type 1 mice. Front. Cell. Neurosci. 16, 998408. https://doi.org/10.3389/fncel.2022.998408.

Byrne, R.A.J., Torvell, M., Daskoulidou, N., Fathalla, D., Kokkali, E., Carpanini, S.M., Morgan, B.P., 2021. Novel monoclonal antibodies against mouse C1q: characterisation and development of a quantitative ELISA for mouse C1q. Mol. Neurobiol. 58, 4323–4336. https://doi.org/10.1007/s12035-021-02419-5.

Callicott, J.H., Mattay, V.S., Verchinski, B.A., Marenco, S., Egan, M.F., Weinberger, D.R., 2003. Complexity of prefrontal cortical dysfunction in schizophrenia: more than up or down. AJP 160, 2209–2215. https://doi.org/10.1176/appi.ajp.160.12.2209.

Carpanini, S.M., Torvell, M., Bevan, R.J., Byrne, R.A.J., Daskoulidou, N., Saito, T., Saido, T.C., Taylor, P.R., Hughes, T.R., Zelek, W.M., Morgan, B.P., 2022. Terminal complement pathway activation drives synaptic loss in Alzheimer's disease models. Acta Neuropathol. Commun. 10, 1–16. https://doi.org/10.1186/S40478-022-01404-W/FIGURES/5.

Comer, A.L., Jinadasa, T., Sriram, B., Phadke, R.A., Kretsge, L.N., Nguyen, T.P.H., Antognetti, G., Gilbert, J.P., Lee, J., Newmark, E.R., Hausmann, F.S., Rosenthal, S.A., Liu Kot, K., Liu, Y., Yen, W.W., Dejanovic, B., Cruz-Martín, A., 2020. Increased expression of schizophrenia-associated gene C4 leads to hypoconnectivity of prefrontal cortex and reduced social interaction. PLoS Biol. 18. https://doi.org/10.1371/journal.pbio.3000604.

Dejanovic, B., Wu, T., Tsai, M.-C., Graykowski, D., Gandham, V.D., Rose, C.M., Bakalarski, C.E., Ngu, H., Wang, Y., Pandey, S., Rezzonico, M.G., Friedman, B.A., Edmonds, R., De Mazière, A., Rakosi-Schmidt, R., Singh, T., Klumperman, J., Foreman, O., Chang, M.C., Xie, L., Sheng, M., Hanson, J.E., 2022. Complement C1q-dependent excitatory and inhibitory synapse elimination by astrocytes and microglia in Alzheimer's disease mouse models. Nat. Aging 2, 837–850. https://doi.org/10.1038/s43587-022-00281-1.

Ermis Akyuz, E., Bell, S.M., 2022. The diverse role of CUB and sushi multiple domains 1 (CSMD1) in human diseases. Genes 13, 2332. https://doi.org/10.3390/genes13122332.

Escudero-Esparza, A., Kalchishkova, N., Kurbasic, E., Jiang, W.G., Blom, A.M., 2013. The novel complement inhibitor human CUB and Sushi multiple domains 1 (CSMD1) protein promotes factor I-mediated degradation of C4b and C3b and inhibits the membrane attack complex assembly. FASEB J. 27, 5083–5093. https://doi.org/10.1096/fj.13-230706.

Feinberg, I., 1982. Schizophrenia: caused by a fault in programmed synaptic elimination during adolescence? J. Psychiatr. Res. 17, 319–334. https://doi.org/10.1016/0022-3956(82)90038-3.

Gialeli, C., Tuysuz, E.C., Staaf, J., Guleed, S., Paciorek, V., Mörgelin, M., Papadakos, K.S., Blom, A.M., 2021. Complement inhibitor CSMD1 modulates epidermal growth factor receptor oncogenic signaling and sensitizes breast cancer cells to chemotherapy. J. Exp. Clin. Cancer Res. 40, 258. https://doi.org/10.1186/s13046-021-02042-1.

Habib, N., McCabe, C., Medina, S., Varshavsky, M., Kitsberg, D., Dvir-Szternfeld, R., Green, G., Dionne, D., Nguyen, L., Marshall, J.L., Chen, F., Zhang, F., Kaplan, T., Regev, A., Schwartz, M., 2020. Disease-associated astrocytes in Alzheimer's disease and aging. Nat. Neurosci. 23, 701–706. https://doi.org/10.1038/s41593-020-0624-8.

Harris, C.L., Hughes, C.E., Williams, A.S., Goodfellow, I., Evans, D.J., Caterson, B., Morgan, B.P., 2003. Generation of anti-complement "prodrugs": cleavable reagents for specific delivery of complement regulators to disease sites. J. Biol. Chem. 278, 36068–36076. https://doi.org/10.1074/jbc.M306351200.

Harris, C.L., Lublin, D.M., Morgan, B.P., 2002a. Efficient generation of monoclonal antibodies for specific protein domains using recombinant immunoglobulin fusion proteins: Pitfalls and solutions. J. Immunol. Methods 268, 245–258. https://doi.org/10.1016/S0022-1759(02)00207-7.

Harris, C.L., Williams, A.S., Linton, S.M., Morgan, B.P., 2002b. Coupling complement regulators to immunoglobulin domains generates effective anti-complement reagents with extended half-life *in vivo*. Clin. Exp. Immunol. 129, 198–207. https://doi.org/10.1046/j.1365-2249.2002.01924.x.

Heinen, S., Hartmann, A., Lauer, N., Wiehl, U., Dahse, H.M., Schirmer, S., Gropp, K., Enghardt, T., Wallich, R., Hälbich, S., Mihlan, M., Schlötzer-Schrehardt, U., Zipfel, P. F., Skerka, C., 2009. Factor H-related protein 1 (CFHR-1) inhibits complement C5 convertase activity and terminal complex formation. Blood 114, 2439–2447. https://doi.org/10.1182/blood-2009-02-205641.

Hong, S., Beja-Glasser, V.F., Nfonoyim, B.M., Frouin, A., Li, S., Ramakrishnan, S., Merry, K.M., Shi, Q., Rosenthal, A., Barres, B.A., Lemere, C.A., Selkoe, D.J., Stevens, B., 2016. Complement and microglia mediate early synapse loss in Alzheimer mouse models. Science 352, 712–716. https://doi.org/10.1126/science:aad8373.

Karlsson, M., Zhang, C., Méar, L., Zhong, W., Digre, A., Katona, B., Sjöstedt, E., Butler, L., Odeberg, J., Dusart, P., Edfors, F., Oksvold, P., von Feilitzen, K., Zwahlen, M., Arif, M., Altay, O., Li, X., Ozcan, M., Mardinoglu, A., Fagerberg, L., Mulder, J., Luo, Y., Ponten, F., Uhlén, M., Lindskog, C., 2021. A single–cell type transcriptomics map of human tissues. Sci. Adv. 7, eabh2169. https://doi.org/10.1126/sciadv.abh2169.

Kraus, D.M., Elliott, G.S., Chute, H., Horan, T., Pfenninger, K.H., Sanford, S.D., Foster, S., Scully, S., Welcher, A.A., Holers, V.M., 2006. CSMD1 is a novel multiple domain complement-regulatory protein highly expressed in the central nervous system and epithelial tissues. J. Immunol. 176, 4419–4430. https://doi.org/10.4049/jimmunol.176.7.4419.

Lee, A.S., Rusch, J., Lima, A.C., Usmani, A., Huang, N., Lepamets, M., Vigh-Conrad, K.A., Worthington, R.E., Mägi, R., Wu, X., Aston, K.I., Atkinson, J.P., Carrell, D.T., Hess, R. A., O'Bryan, M.K., Conrad, D.F., 2019. Rare mutations in the complement regulatory gene CSMD1 are associated with male and female infertility. Nat. Commun. 10. https://doi.org/10.1038/s41467-019-12522-w.

Li, J., Khankan, R.R., Caneda, C., Godoy, M.I., Haney, M.S., Krawczyk, M.C., Bassik, M. C., Sloan, S.A., Zhang, Y., 2019. Astrocyte-to-astrocyte contact and a positive feedback loop of growth factor signaling regulate astrocyte maturation. Glia 67, 1571–1597. https://doi.org/10.1002/glia.23630.

Li, X., Lee, N.K., Ye, Y.W., Waber, P.G., Schweitzer, C., Cheng, Q.C., Nisen, P.D., 1994. Allelic loss at chromosomes 3p, 8p, 13q, and l7p associated with poor prognosis in head and neck cancer. J. Natl Cancer Inst. 86, 1524–1529. https://doi.org/10.1093/jnci/86.20.1524.

Maguire, E., Menzies, G.E., Phillips, T., Sasner, M., Williams, H.M., Czubala, M.A., Evans, N., Cope, E.L., Sims, R., Howell, G.R., Lloyd-Evans, E., Williams, J., Allen, N. D., Taylor, P.R., 2021. PIP2 depletion and altered endocytosis caused by expression of Alzheimer's disease-protective variant PLCγ2 R522. EMBO J. 40, e105603. https://doi.org/10.15252/embj.2020105603.

Michelfelder, S., Fischer, F., Wäldin, A., Hörle, K.V., Pohl, M., Parsons, J., Reski, R., Decker, E.L., Zipfel, P.F., Skerka, C., Häffner, K., 2018. The MFHR1 fusion protein is a novel synthetic multitarget complement inhibitor with therapeutic potential. J. Am. Soc. Nephrol. 29, 1141. https://doi.org/10.1681/ASN.2017070738.

Nilsson, B., Nilsson, U.R., 1986. Antigens of complement factor C3 involved in the interactions with factors I and H. Scand. J. Immunol. 23, 357–363. https://doi.org/10.1111/j.1365-3083.1986.tb01976.x.

Notter, T., 2021. Astrocytes in Schizophrenia. Brain Neurosci. Adv. 5, 23982128211009148. https://doi.org/10.1177/23982128211009148.

Ojha, H., Ghosh, P., Singh Panwar, H., Shende, R., Gondane, A., Mande, S.C., Sahu, A., 2019. Spatially conserved motifs in complement control protein domains determine functionality in regulators of complement activation-family proteins. Commun. Biol. 2. https://doi.org/10.1038/s42003-019-0529-9.

Pardiñas, A.F., Holmans, P., Pocklington, A.J., Escott-Price, V., Ripke, S., Carrera, N., Legge, S.E., Bishop, S., Cameron, D., Hamshere, M.L., Han, J., Hubbard, L., Lynham, A., Mantripragada, K., Rees, E., MacCabe, J.H., McCarroll, S.A., Baune, B. T., Breen, G., Byrne, E.M., Dannlowski, U., Eley, T.C., Hayward, C., Martin, N.G., McIntosh, A.M., Plomin, R., Porteous, D.J., Wray, N.R., Caballero, A., Geschwind, D. H., Huckins, L.M., Ruderfer, D.M., Santiago, E., Sklar, P., Stahl, E.A., Won, H., Agerbo, E., Als, T.D., Andreassen, O.A., Bækvad-Hansen, M., Mortensen, P.B., Pedersen, C.B., Børglum, A.D., Bybjerg-Grauholm, J., Djurovic, S., Durmishi, N., Pedersen, M.G., Golimbet, V., Grove, J., Hougaard, D.M., Mattheisen, M., Molden, E., Mors, O., Nordentoft, M., Pejovic-Milovancevic, M., Sigurdsson, E., Silagadze, T., Hansen, C.S., Stefansson, K., Stefansson, H., Steinberg, S., Tosato, S., Werge, T., Harold, D., Sims, R., Gerrish, A., Chapman, J., Abraham, R., Hollingworth, P., Pahwa, J., Denning, N., Thomas, C., Taylor, S., Powell, J., Proitsi, P., Lupton, M., Lovestone, S., Passmore, P., Craig, D., McGuinness, B., Johnston, J., Todd, S., Maier, W., Jessen, F., Heun, R., Schurmann, B., Ramirez, A., Becker, T., Herold, C., Lacour, A., Drichel, D., Nothen, M., Goate, A., Cruchaga, C., Nowotny, P., Morris, J. C., Mayo, K., O'Donovan, M., Owen, M., Williams, J., Achilla, E., Barr, C.L., Böttger, T.W., Cohen, D., Curran, S., Dempster, E., Dima, D., Sabes-Figuera, R., Flanagan, R.J., Frangou, S., Frank, J., Gasse, C., Gaughran, F., Giegling, I., Hannon, E., Hartmann, A.M., Heißerer, B., Helthuis, M., Horsdal, H.T., Ingimarsson, O., Jollie, K., Kennedy, J.L., Köhler, O., Konte, B., Lang, M., Lewis, C., MacCaba, J., Malhotra, A.K., McCrone, P., Meier, S.M., Mill, J., Nöthen, M.M., Pedersen, C.B., Rietschel, M., Rujescu, D., Schwalber, A., Sørensen, H.J., Spencer, B., Støvring, H., Strohmaier, J., Sullivan, P., Vassos, E., Verbelen, M., Collier, D.A., Kirov, G., Owen, M.J., O'Donovan, M.C., Walters, J.T.R., 2018. Common schizophrenia alleles are enriched in mutation-intolerant genes and in regions under strong background selection. Nat. Genet. 50, 381–389. https://doi.org/10.1038/s41588-018-0059-2.

Phadke, R.A., Brack, A., Fournier, L.A., Kruzich, E., Sha, M., Picard, I., Johnson, C., Stroumbakis, D., Salgado, M., Yeung, C., Escude Velasco, B., Liu, Y.Y., Cruz-Martín, A., 2024. The schizophrenia risk gene C4 induces pathological synaptic loss by impairing AMPAR trafficking. Mol Psychiatry 4, 1–14. https://doi.org/10.1038/s41380-024-02701-7.

Phillips, M.L., Mi-Hua, T., Morrison, S.L., Schumaker, V.N., 1994. Human/mouse chimeric monoclonal antibodies with human IgG1, IgG2, IgG3 and IgG4 constant domains: electron microscopic and hydrodynamic characterization. Mol. Immunol. 31, 1201–1210. https://doi.org/10.1016/0161-5890(94)90034-5.

Ripke, S., O'Dushlaine, C., Chambert, K., Moran, J.L., Kähler, A.K., Akterin, S., Bergen, S. E., Collins, A.L., Crowley, J.J., Fromer, M., Kim, Y., Lee, S.H., Magnusson, P.K.E., Sanchez, N., Stahl, E.A., Williams, S., Wray, N.R., Xia, K., Bettella, F., Borglum, A.D., Bulik-Sullivan, B.K., Cormican, P., Craddock, N., De Leeuw, C., Durmishi, N., Gill, M., Golimbet, V., Hamshere, M.L., Holmans, P., Hougaard, D.M., Kendler, K.S., Lin, K., Morris, D.W., Mors, O., Mortensen, P.B., Neale, B.M., O'Neill, F.A., Owen, M. J., Milovancevic, M.P., Posthuma, D., Powell, J., Richards, A.L., Riley, B.P., Ruderfer, D., Sigurdsson, E., Silagadze, T., Smit, A.B., Stefansson, H., Steinberg, S., Suvisaari, J., Tosato, S., Verhage, M., Walters, J.T., Levinson, D.F., Gejman, P.V., Laurent, C., Mowry, B.J., O'Donovan, M.C., Pulver, A.E., Schwab, S.G., Wildenauer, D.B., Dudbridge, F., Shi, J., Albus, M., Alexander, M., Campion, D., Cohen, D., Dikeos, D., Duan, J., Eichhammer, P., Godard, S., Hansen, M., Lerer, F.B., Liang, K.Y., Maier, W., Mallet, J., Nertney, D.A., Nestadt, G., Norton, N., Papadimitriou, G.N., Ribble, R., Sanders, A.R., Silverman, J.M., Walsh, D., Williams, N.M., Wormley, B., Arranz, M.J., Bakker, S., Bender, S., Bramon, E., Collier, D., Crespo-Facorro, B., Hall, J., Iyegbe, C., Jablensky, A., Kahn, R.S., Kalaydjieva, L., Lawrie, S., Lewis, C.M., Linszen, D.H., Mata, I., McIntosh, A., Murray, R.M., Ophoff, R.A., Rujescu, D., Van Os, J., Walshe, M., Weisbrod, M., Wiersma, D., Donnelly, P., Blackwell, J.M., Brown, M.A., Casas, J.P., Corvin, A.P., Duncanson, A., Jankowski, J., Markus, H.S., Mathew, C.G., Palmer, C.N.A., Plomin, R., Rautanen, A., Sawcer, S.J., Trembath, R.C., Viswanathan, A.C., Wood, N. W., Spencer, C.C.A., Band, G., Bellenguez, C., Freeman, C., Hellenthal, G., Giannoulatou, E., Pirinen, M., Pearson, R.D., Strange, A., Su, Z., Vukcevic, D., Langford, C., Hunt, S.E., Edkins, S., Gwilliam, R., Blackburn, H., Bumpstead, S.J., Dronov, S., Gillman, M., Gray, E., Hammond, N., Jayakumar, A., McCann, O.T., Liddle, J., Potter, S.C., Ravindrarajah, R., Ricketts, M., Tashakkori-Ghanbaria, A., Waller, M.J., Weston, P., Widaa, S., Whittaker, P., Barroso, I., Deloukas, P., McCarthy, M.I., Stefansson, K., Scolnick, E., Purcell, S., McCarroll, S.A., Sklar, P., Hultman, C.M., Sullivan, P.F., 2013. Genome-wide association analysis identifies 13 new risk loci for schizophrenia. Nat. Genet. 45, 1150–1159. https://doi.org/10.1038/ng.2742.

Ruseva, M.M., Heurich, M. 2014. Purification and Characterization of Human and Mouse Complement C3, in: Gadjeva, M. (Ed.), The Complement System: Methods and Protocols. Humana Press, Totowa, NJ, pp. 75–91. https://doi.org/10.1007/978-1-62703-724-2_6.

Saunders, A., Macosko, E.Z., Wysoker, A., Goldman, M., Krienen, F.M., de Rivera, H., Bien, E., Baum, M., Bortolin, L., Wang, S., Goeva, A., Nemesh, J., Kamitaki, N., Brumbaugh, S., Kulp, D., McCarroll, S.A., 2018. Molecular diversity and specializations among the cells of the adult mouse brain. Cell 174, 1015–1030.e16. https://doi.org/10.1016/j.cell.2018.07.028.

Schafer, D.P., Lehrman, E.K., Kautzman, A.G., Koyama, R., Mardinly, A.R., Yamasaki, R., Ransohoff, R.M., Greenberg, M.E., Barres, B.A., Stevens, B., 2012. Microglia sculpt postnatal neural circuits in an activity and complement-dependent manner. Neuron 74, 691–705. https://doi.org/10.1016/j.neuron.2012.03.026.

Schartz, N.D., Liang, H.Y., Carvalho, K., Chu, S.-H., Mendoza-Arvilla, A., Petrisko, T.J., Gomez-Arboledas, A., Mortazavi, A., Tenner, A.J., 2024. C5aR1 antagonism suppresses inflammatory glial responses and alters cellular signaling in an Alzheimer's disease mouse model. Nat. Commun. 15, 7028. https://doi.org/10.1038/s41467-024-51163-6.

Schizophrenia Working Group of the Psychiatric Genomics Consortium, 2014. Biological insights from 108 schizophrenia-associated genetic loci. Nature 511, 421–427. https://doi.org/10.1038/nature13595.

Schmidt, C.Q., Lambris, J.D., Ricklin, D., 2016. Protection of host cells by complement regulators. Immunol. Rev. 274, 152–171. https://doi.org/10.1111/imr.12475.

Scholnick, S.B., Haughey, B.H., Sunwoo, J.B., El-Mofty, S.K., Baty, J.D., Piccirillo, J.F., Zequeira, M.R., 1996. Chromosome 8 allelic loss and the outcome of patients with squamous cell carcinoma of the supraglottic larynx. J. Natl. Cancer Inst. 88, 1676–1682. https://doi.org/10.1093/jnci/88.22.1676.

Sekar, A., Bialas, A.R., De Rivera, H., Davis, A., Hammond, T.R., Kamitaki, N., Tooley, K., Presumey, J., Baum, M., Van Doren, V., Genovese, G., Rose, S.A., Handsaker, R.E., Daly, M.J., Carroll, M.C., Stevens, B., McCarroll, S.A., 2016. Schizophrenia risk from complex variation of complement component 4. Nature 530, 177–183. https://doi.org/10.1038/nature16549.

Sellgren, C.M., Gracias, J., Watmuff, B., Biag, J.D., Thanos, J.M., Whittredge, P.B., Fu, T., Worringer, K., Brown, H.E., Wang, J., Kaykas, A., Karmacharya, R., Goold, C.P., Sheridan, S.D., Perlis, R.H., 2019. Increased synapse elimination by microglia in schizophrenia patient-derived models of synaptic pruning. Nat. Neurosci. 22, 374–385. https://doi.org/10.1038/s41593-018-0334-7.

Serio, A., Bilican, B., Barmada, S.J., Ando, D.M., Zhao, C., Siller, R., Burr, K., Haghi, G., Story, D., Nishimura, A.L., Carrasco, M.A., Phatnani, H.P., Shum, C., Wilmut, I., Maniatis, T., Shaw, C.E., Finkbeiner, S., Chandran, S., 2013. Astrocyte pathology and the absence of non-cell autonomy in an induced pluripotent stem cell model of TDP-43 proteinopathy. Proc. Natl. Acad. Sci. 110, 4697–4702. https://doi.org/10.1073/pnas.1300398110.

Shi, Q., Chowdhury, S., Ma, R., Le, K.X., Hong, S., Caldarone, B.J., Stevens, B., Lemere, C. A., 2017. Complement C3 deficiency protects against neurodegeneration in aged plaque-rich APP/PS1 mice. Sci. Transl. Med. 9. https://doi.org/10.1126/scitranslmed.aaf6295.

Shi, Y., Kirwan, P., Livesey, F.J., 2012. Directed differentiation of human pluripotent stem cells to cerebral cortex neurons and neural networks. Nat. Protoc. 7, 1836–1846. https://doi.org/10.1038/nprot.2012.116.

Smith, R., Dodd, I., Oldroyd, R., Harry, J., Clarke, C., Rolan, P., Dawes, L., 2001. Preclinical and clinical progression of a membrane-targeted complement regulator therapeutic. Mol. Immunol. 38, 122.

Steen, V.M., Nepal, C., Ersland, K.M., Holdhus, R., Nævdal, M., Ratvik, S.M., Skrede, S., Håvik, B., 2013. Neuropsychological deficits in mice depleted of the schizophrenia susceptibility gene CSMD1. PLoS One 8. https://doi.org/10.1371/journal.pone.0079501.

Stevens, B., Allen, N.J., Vazquez, L.E., Howell, G.R., Christopherson, K.S., Nouri, N., Micheva, K.D., Mehalow, A.K., Huberman, A.D., Stafford, B., Sher, A., Litke, A.M.M., Lambris, J.D., Smith, S.J., John, S.W.M., Barres, B.A., 2007. The classical complement cascade mediates CNS synapse elimination. Cell 131, 1164–1178. https://doi.org/10.1016/j.cell.2007.10.036.

The Schizophrenia Psychiatric Genome-Wide Association Study (GWAS) Consortium, 2011. Genome-wide association study identifies five new schizophrenia loci. Nat. Genet. 43, 969–978. https://doi.org/10.1038/ng.940.

Trubetskoy, V., Pardiñas, A.F., Qi, T., Panagiotaropoulou, G., Awasthi, S., Bigdeli, T.B., Bryois, J., Chen, C.-Y., Dennison, C.A., Hall, L.S., Lam, M., Watanabe, K., Frei, O., Ge, T., Harwood, J.C., Koopmans, F., Magnusson, S., Richards, A.L., Sidorenko, J., Wu, Y., Zeng, J., Grove, J., Kim, M., Li, Z., Voloudakis, G., Zhang, W., Adams, M., Agartz, I., Atkinson, E.G., Agerbo, E., Al Eissa, M., Albus, M., Alexander, M., Alizadeh, B.Z., Alptekin, K., Als, T.D., Amin, F., Arolt, V., Arrojo, M., Athanasiu, L., Azevedo, M.H., Bacanu, S.A., Bass, N.J., Begemann, M., Belliveau, R.A., Bene, J., Benyamin, B., Bergen, S.E., Blasi, G., Bobes, J., Bonassi, S., Braun, A., Bressan, R.A., Bromet, E.J., Bruggeman, R., Buckley, P.F., Buckner, R.L., Bybjerg-Grauholm, J., Cahn, W., Cairns, M.J., Calkins, M.E., Carr, V.J., Castle, D., Catts, S.V., Chambert, K. D., Chan, R.C.K., Chaumette, B., Cheng, W., Cheung, E.F.C., Chong, S.A., Cohen, D., Consoli, A., Cordeiro, Q., Costas, J., Curtis, C., Davidson, M., Davis, K.L., de Haan, L., Degenhardt, F., DeLisi, L.E., Demontis, D., Dickerson, F., Dikeos, D., Dinan, T., Djurovic, S., Duan, J., Ducci, G., Dudbridge, F., Eriksson, J.G., Fañanás, L., Faraone, S.V., Fiorentino, A., Forstner, A., Frank, J., Freimer, N.B., Fromer, M., Frustaci, A., Gadelha, A., Genovese, G., Gershon, E.S., Giannitelli, M., Giegling, I., Giusti-Rodríguez, P., Godard, S., Goldstein, J.I., González Peñas, J., González-Pinto, A., Gopal, S., Gratten, J., Green, M.F., Greenwood, T.A., Guillin, O., Gülöksüz, S., Gur, R.E., Gur, R.C., Gutiérrez, B., Hahn, E., Hakonarson, H., Haroutunian, V., Hartmann, A.M., Harvey, C., Hayward, C., Henskens, F.A., Herms, S., Hoffmann, P., Howrigan, D.P., Ikeda, M., Iyegbe, C., Joa, I., Julià, A., Kähler, A.K., Kam-Thong, T., Kamatani, Y., Karachanak-Yankova, S., Kebir, O., Keller, M.C., Kelly, B.J., Khrunin, A., Kim, S.-W., Klovins, J., Kondratiev, N., Konte, B., Kraft, J., Kubo, M., Kučinskas, V., Kučinskiene, Z.A., Kusumawardhani, A., Kuzelova-Ptackova, H., Landi, S., Lazzeroni, L.C., Lee, P.H., Legge, S.E., Lehrer, D.S., Lencer, R., Lerer, B., Li, M., Lieberman, J., Light, G.A., Limborska, S., Liu, C.-M., Lönnqvist, J., Loughland, C.M., Lubinski, J., Luykx, J.J., Lynham, A., Macek, M., Mackinnon, A., Magnusson, P.K.E., Maher, B.S., Maier, W., Malaspina, D., Mallet, J., Marder, S.R., Marsal, S., Martin, A.R., Martorell, L., Mattheisen, M., McCarley, R.W., McDonald, C., McGrath, J.J., Medeiros, H., Meier, S., Melegh, B., Melle, I., Mesholam-Gately, R.I., Metspalu, A., Michie, P.T., Milani, L., Milanova, V., Mitjans, M., Molden, E., Molina, E., Molto, M.D., Mondelli, V., Moreno, C., Morley, C.P., Muntané, G., Murphy, K.C., Myin-Germeys, I., Nenadić, I., Nestadt, G., Nikitina-Zake, L., Noto, C., Nuechterlein, K.H., O'Brien, N.L., O'Neill, F.A., Oh, S.-Y., Olincy, A., Ota, V.K., Pantelis, C., Papadimitriou, G.N., Parellada, M., Paunio, T., Pellegrino, R., Periyasamy, S., Perkins, D.O., Pfuhlmann, B., Pietiläinen, O., Pimm, J., Porteous, D., Powell, J., Quattrone, D., Quested, D., Radant, A.D., Rampino, A., Rapaport, M.H., Rautanen, A., Reichenberg, A., Roe, C., Roffman, J.L., Roth, J., Rothermundt, M., Rutten, B.P.F., Saker-Delye, S., Salomaa, V., Sanjuan, J., Santoro, M.L., Savitz, A., Schall, U., Scott, R.J., Seidman, L.J., Sharp, S.I., Shi, J., Siever, L.J., Sigurdsson, E., Sim, K., Skarabis, N., Slominsky, P., So, H.-C., Sobell, J. L., Söderman, E., Stain, H.J., Steen, N.E., Steixner-Kumar, A.A., Stögmann, E., Stone, W.S., Straub, R.E., Streit, F., Strengman, E., Stroup, T.S., Subramaniam, M., Sugar, C.A., Suvisaari, J., Svrakic, D.M., Swerdlow, N.R., Szatkiewicz, J.P., Ta, T.M. T., Takahashi, A., Terao, C., Thibaut, F., Toncheva, D., Tooney, P.A., Torretta, S., Tosato, S., Tura, G.B., Turetsky, B.I., Üçok, A., Vaaler, A., van Amelsvoort, T., van Winkel, R., Veijola, J., Waddington, J., Walter, H., Waterreus, A., Webb, B.T., Weiser, M., Williams, N.M., Witt, S.H., Wormley, B.K., Wu, J.Q., Xu, Z., Yolken, R., Zai, C.C., Zhou, W., Zhu, F., Zimprich, F., Atbaşoğlu, E.C., Ayub, M., Benner, C., Bertolino, A., Black, D.W., Bray, N.J., Breen, G., Buccola, N.G., Byerley, W.F., Chen, W.J., Cloninger, C.R., Crespo-Facorro, B., Donohoe, G., Freedman, R., Galletly, C., Gandal, M.J., Gennarelli, M., Hougaard, D.M., Hwu, H.-G., Jablensky, A. V., McCarroll, S.A., Moran, J.L., Mors, O., Mortensen, P.B., Müller-Myhsok, B., Neil, A.L., Nordentoft, M., Pato, M.T., Petryshen, T.L., Pirinen, M., Pulver, A.E., Schulze, T.G., Silverman, J.M., Smoller, J.W., Stahl, E.A., Tsuang, D.W., Vilella, E., Wang, S.-H., Xu, S., Dai, N., Wenwen, Q., Wildenauer, D.B., Agiananda, F., Amir, N., Antoni, R., Arsianti, T., Asmarahadi, A., Diatri, H., Djatmiko, P., Irmansyah, I., Khalimah, S., Kusumadewi, I., Kusumaningrum, P., Lukman, P.R., Nasrun, M.W., Safyuni, N.S., Prasetyawan, P., Semen, G., Siste, K., Tobing, H., Widiasih, N., Wiguna, T., Wulandari, D., Evalina, N., Hananto, A.J., Ismoyo, J.H., Marini, T.M., Henuhili, S., Reza, M., Yusnadewi, S., Abyzov, A., Akbarian, S., Ashley-Koch, A., van Bakel, H., Breen, M., Brown, M., Bryois, J., Carlyle, B., Charney, A., Coetzee, G., Crawford, G., Dracheva, S., Emani, P., Farnham, P., Fromer, M., Galeev, T., Gandal, M., Gerstein, M., Giase, G., Girdhar, K., Goes, F., Grennan, K., Gu, M., Guerra, B., Gursoy, G., Hoffman, G., Hyde, T., Jaffe, A., Jiang, S., Jiang, Y., Kefi, A., Kim, Y., Kitchen, R., Knowles, J.A., Lay, F., Lee, D., Li, M., Liu, C., Liu, S., Mattei, E., Navarro, F., Pan, X., Peters, M.A., Pinto, D., Pochareddy, S., Polioudakis, D., Purcaro, M., Purcell, S., Pratt, H., Reddy, T., Rhie, S., Roussos, P., Rozowsky, J., Sanders, S., Sestan, N., Sethi, A., Shi, X., Shieh, A., Swarup, V., Szekely, A., Wang, D., Warrell, J., Weissman, S., Weng, Z., White, K., Wiseman, J., Witt, H., Won, H., Wood, S., Wu, F., Xu, X., Yao, L., Zandi, P., Arranz, M.J., Bakker, S., Bender, S., Bramon, E., Collier, D.A., Crepo-Facorro, B., Hall, J., Iyegbe, C., Kahn, R., Lawrie, S., Lewis, C., Lin, K., Linszen, D.H., Mata, I., McIntosh, A., Murray, R.M., Ophoff, R.A., van Os, J., Powell, J., Rujescu, D., Walshe, M., Weisbrod, M., Achsel, T., Andres-Alonso, M., Bagni, C., Bayés, À., Biederer, T., Brose, N., Brown, T.C., Chua, J.J.E., Coba, M.P., Cornelisse, L.N., de Jong, A.P.H., de Juan-Sanz, J., Dieterich, D.C., Feng, G., Goldschmidt, H.L., Gundelfinger, E.D., Hoogenraad, C., Huganir, R.L., Hyman, S.E., Imig, C., Jahn, R., Jung, H., Kaeser, P.S., Kim, E., Koopmans, F., Kreutz, M.R., Lipstein, N., MacGillavry, H.D., Malenka, R., McPherson, P.S., O'Connor, V., Pielot, R., Ryan, T.A., Sahasrabudhe, D., Sala, C., Sheng, M., Smalla, K.-H., Smit, A.B., Südhof, T.C., Thomas, P.D., Toonen, R.F., van Weering, J. R.T., Verhage, M., Verpelli, C., Adolfsson, R., Arango, C., Baune, B.T., Belangero, S.I., Børglum, A.D., Braff, D., Bramon, E., Buxbaum, J.D., Campion, D., Cervilla, J.A., Cichon, S., Collier, D.A., Corvin, A., Curtis, D., Forti, M.D., Domenici, E., Ehrenreich, H., Escott-Price, V., Esko, T., Fanous, A.H., Gareeva, A., Gawlik, M., Gejman, P.V., Gill, M., Glatt, S.J., Golimbet, V., Hong, K.S., Hultman, C.M., Hyman, S.E., Iwata, N., Jönsson, E.G., Kahn, R.S., Kennedy, J.L., Khusnutdinova, E., Kirov, G., Knowles, J.A., Krebs, M.-O., Laurent-Levinson, C., Lee, J., Lencz, T., Levinson, D.F., Li, Q.S., Liu, J., Malhotra, A.K., Malhotra, D., McIntosh, A., McQuillin, A., Menezes, P.R., Morgan, V.A., Morris, D.W., Mowry, B.J., Murray, R. M., Nimgaonkar, V., Nöthen, M.M., Ophoff, R.A., Paciga, S.A., Palotie, A., Pato, C.N., Qin, S., Rietschel, M., Riley, B.P., Rivera, M., Rujescu, D., Saka, M.C., Sanders, A.R., Schwab, S.G., Serretti, A., Sham, P.C., Shi, Y., St Clair, D., Stefánsson, H., Stefansson, K., Tsuang, M.T., van Os, J., Vawter, M.P., Weinberger, D.R., Werge, T., Wildenauer, D.B., Yu, X., Yue, W., Holmans, P.A., Pocklington, A.J., Roussos, P., Vassos, E., Verhage, M., Visscher, P.M., Yang, J., Posthuma, D., Andreassen, O.A., Kendler, K.S., Owen, M.J., Wray, N.R., Daly, M.J., Huang, H., Neale, B.M., Sullivan, P.F., Ripke, S., Walters, J.T.R., O'Donovan, M.C., de Haan, L., van Amelsvoort, T., van Winkel, R., Gareeva, A., Sham, P.C., Shi, Y., St Clair, D., van Os, J., 2022. Mapping genomic loci implicates genes and synaptic biology in schizophrenia. Nature 604, 502–508. https://doi.org/10.1038/s41586-022-04434-5.

Tzioras, M., Daniels, M.J.D., Davies, C., Baxter, P., King, D., McKay, S., Varga, B., Popovic, K., Hernandez, M., Stevenson, A.J., Barrington, J., Drinkwater, E., Borella, J., Holloway, R.K., Tulloch, J., Moss, J., Latta, C., Kandasamy, J., Sokol, D., Smith, C., Miron, V.E., Káradóttir, R.T., Hardingham, G.E., Henstridge, C.M., Brennan, P.M., McColl, B.W., Spires-Jones, T.L., 2023. Human astrocytes and microglia show augmented ingestion of synapses in Alzheimer's disease via MFG-E8. Cell Rep. Med. 4, 101175. https://doi.org/10.1016/j.xcrm.2023.101175.

Vanderpuye, O.A., Beville, C.M., McIntyre, J.A., 1994. Characterization of cofactor activity for factor I: Cleavage of complement C4 in human syncytiotrophoblast microvilli. Placenta 15, 157–170. https://doi.org/10.1016/S0143-4004(05)80452-7.

Wu, T., Dejanovic, B., Gandham, V.D., Gogineni, A., Edmonds, R., Schauer, S., Srinivasan, K., Huntley, M.A., Wang, Y., Wang, T.M., Hedehus, M., Barck, K.H., Stark, M., Ngu, H., Foreman, O., Meilandt, W.J., Elstrott, J., Chang, M.C., Hansen, D. V., Carano, R.A.D., Sheng, M., Hanson, J.E., 2019. Complement C3 Is activated in human AD brain and is required for neurodegeneration in mouse models of amyloidosis and tauopathy. Cell Rep. 28, 2111–2123. https://doi.org/10.1016/j.celrep.2019.07.060.

Yilmaz, M., Yalcin, E., Presumey, J., Aw, E., Ma, M., Whelan, C.W., Stevens, B., McCarroll, S.A., Carroll, M.C., 2021. Overexpression of schizophrenia susceptibility factor human complement C4A promotes excessive synaptic loss and behavioral changes in mice. Nat. Neurosci. 24, 214–224. https://doi.org/10.1038/s41593-020-00763-8.

Zelek, W.M., Bevan, R.J., Morgan, B.P., 2024a. Targeting terminal pathway reduces brain complement activation, amyloid load and synapse loss, and improves cognition in a mouse model of dementia. Brain Behav. Immun. 118, 355–363. https://doi.org/10.1016/j.bbi.2024.03.017.

Zelek, W.M., Bevan, R.J., Nimmo, J., Dewilde, M., Strooper, B., Morgan, B.P., 2024b. Brain-penetrant complement inhibition mitigates neurodegeneration in an Alzheimer's disease mouse model. Brain 148 (3), e278.

Zelek, W.M., Harris, C.L., Morgan, B.P., 2018a. Extracting the barbs from complement assays: Identification and optimisation of a safe substitute for traditional buffers. Immunobiology 223, 744–749. https://doi.org/10.1016/j.imbio.2018.07.016.

Zelek, W.M., Morgan, B.P., 2020. Monoclonal antibodies capable of inhibiting complement downstream of C5 in multiple species. Front. Immunol. 11, 612402. https://doi.org/10.3389/fimmu.2020.612402.

Zelek, W.M., Stott, M., Walters, D., Harris, C.L., Morgan, B.P., 2018b. Characterizing a pH-switch anti-C5 antibody as a tool for human and mouse complement C5 purification and cross-species inhibition of classical and reactive lysis. Immunology 155, 396–403. https://doi.org/10.1111/imm.12982.

Zelek, W.M., Taylor, P.R., Morgan, B.P., 2019. Development and characterization of novel anti-C5 monoclonal antibodies capable of inhibiting complement in multiple species. Immunology 157, 283–295. https://doi.org/10.1111/imm.13083.